BREMERHAVEN UNIVERSITY OF APPLIED SCIENCES

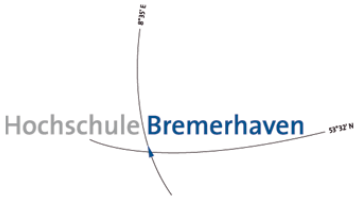

EAFIT UNIVERSITY

APPLICATION OF GAS HYDRATE EQUILIBRIA PREDICTION IN PROCESS ENGINEERING

ANDRES ELOYBAN BONILLA VELLOJIN

(Student Code Bremerhaven Univ.) – 31300

(Student Code EAFIT Univ.) - 200917000004

UNDER SUPERVISION OF:

PROF. DR. – ING. WILFRIED SCHÜTZ

Dr. BASTIAN SCHMID

For the completion of the study course and honor of:

Bachelor of Science in Sustainable Energy and Environmental Technologies of Bremerhaven University of Applied Sciences and Bachelor of Science in Process Engineering of EAFIT University

Declaration

I hereby declare, that I have solely done this work on my own and have not used other sources as reference except for the sources, which are mentioned in this work.

Andres Eloyban Bonilla Vellojin

Bremerhaven 12.05.2014

I would like to take this space to thank all the people that helped me achieve this honor, I will be grateful forever with you and you will be forever in my memories.

First of all, I would like to thank my parents Eloyban Bonilla and Buena Vellojin, without you this couldn't have been possible. You made my dreams become a reality, you gave me all my education and you put me here in Germany to chase my goals. Also, my brothers Mau and Elo and my sister Ofe, I grew up by watching you three, you helped me become what I am today.

I would like to specially thank MSc. Juan David Ortega and Prof. Dr. rer. Nat. habil Katharina Theis-Bröhl for making possible the double degree which allowed me to come to Germany. Also, extend this gratitude to Prof. Dr. Jürgen Gmehling for accepting me in DDBST and giving me the opportunity of making this bachelor work and Prof. Dr.-Ing.Wilfried Schütz for helping me to find this placement. Also, Dr. Bastian Schmid for all his support and help during my bachelor work in DDBST.

I would like to thank all my Professors and lecturers in EAFIT and Bremerhaven University for providing me all the education in order to gain knowledge in all the engineering aspects. Also, the whole DDBST group for their support.

Last but not less, I would like to thank all my friends during my studies in Medellin and Bremerhaven. I would specially thank my Banzai friends in Medellin, Malte and Jose, for always my friends (von eins Alter!); and Susy, thanks for all your support.

29 of April, 2014. Oldenburg, Germany

Andres E. Bonilla V.

ABSTRACT

From almost two centuries gas hydrates have gained an important role in process engineering, due to their economic and environmental impact in the industry. Every day, more companies and engineers gain interest in this topic, as every day new challenges show gas hydrate as a crucial factor, making their study a solution for the oncoming future. Gas hydrates are ice-like cage structures of water host molecules containing guest gas components. They exist naturally in conditions of high pressures and low temperatures, typical and common conditions for some chemical and petrochemical processes [1].

Based on the Ph.D. work of Windmeier [2] and the Ph.D. work of Rock [3], the thermodynamic description of hydrate phases is implemented following the state-of-the-art of science and technology. With the help of the Dortmund Data Bank (DDB) and the corresponding software package (DDBSP) [26], the performance of the method was improved and compared to a large number of published data from all over the world. Also, the application of the hydrate equilibria prediction was studied focused in Process Engineering, with a case study related to the natural gas extraction, production and transport.

It was determined that gas hydrates prediction is crucial for the natural gas process design. Where, for the gas treatment and liquid processing stages no formation is reached, for dehydration a minimum temperature of 290.15 K is critical and for the extraction and transport the use of inhibitors is essential. A 40 mass% of ethylene glycol was found suitable for preventing hydrate formation in the extraction process and 20 mass% of methanol in the pipelines.

GAS HYDRATES, PROCESS ENGINEERING, NATURAL GAS, PSRK, VTPR, LIFAC.

RESUMEN

Desde hace cerca de dos siglos, los hidratos de gas han ganado un rol importante en la ingeniería de procesos, debido a su impacto económico y ambiental en la industria. Cada día, más compañías e ingenieros ganan interés en este tema, a medida que nuevos desafíos muestran a los hidratos de gas como un factor crucial, haciendo su estudio una solución para un futuro próximo. Los gases de hidrato son estructuras similares al hielo, compuestos de moléculas huéspedes de agua conteniendo compuestos gaseosos. Existen naturalmente en condiciones de presiones altas y bajas temperaturas, condiciones típicas de algunos procesos químicos y petroquímicos [1].

Basado en el trabajo doctoral de Windmeier [2] y el trabajo doctoral the Rock [3], la descripción termodinámica de las fases de los hidratos de gas es implementada siguiendo el estado del arte de la ciencia y la tecnología. Con ayuda del Dortmund Data Bank (DDB) y el paquete de software correspondiente (DDBSP) [26], el desempeño del método fue mejorado y comparado con una gran cantidad de datos publicados alrededor del mundo. También, la aplicabilidad de la predicción de los hidratos de gas fue estudiada enfocada en la ingeniería de procesos, con un caso de estudio relacionado con la extracción, producción y transporte del gas natural.

Fue determinado que la predicción de los hidratos de gas es crucial en el diseño del proceso del gas natural. Donde, en las etapas de tratamiento del gas y procesamiento de líquido no se presenta ninguna formación, en la etapa de deshidratación una temperatura mínima de 290.15 K es crítica y para la extracción y transporte el uso de inhibidores es esencial. Una composición másica de 40% de etilenglicol fue encontrada apropiada para prevenir la formación de hidrato de gas en la extracción y una composición másica de 20% de metanol en el transporte.

HIDRATOS DE GAS, INGENIERIA DE PROCESOS, GAS NATURAL, PSRK, VTPR, LIFAC

INDEX

TABLES INDEX

FIGURES INDEX

1. INTRODUCTION

1.1. HISTORY

The scientific mention of gas hydrates is attributed to Joseph Priestly in 1778 [1], who, after leaving his laboratory window open to make some cold experiments, the next day saw how SO_2 impregnate water and make it freeze and refreeze. But there are no validation records which support his experiment and it could have been possible that water changed to ice due to temperatures below freezing point. Because of this, the credited as first observance of gas hydrate is given to Davy's discovery of chlorine hydrate in the year 1810 [4]. After this first research, several more researchers started to emerge, making gas hydrate a scientific curiosity of the time. The end of the 19^{th} century was marked by the first studies of hydrocarbon hydrates and a tendency to set an integral number of water molecules per guest. Also, the first plot of a phase equilibrium diagram was made by Roozeboom in 1884, for SO_2 [1].

In 1930 Hammerschmidt determined, that natural gas hydrates were blocking gas transmission lines and not ice as initially thought. Because of this discovery, gas hydrates gained an importance in the industry and engineering field; they were not longer a scientific curiosity but a crucial factor to be studied [5]. An important consequence was the regulation of the water content in pipelines. Also, many researchers investigated the effects of kinetic inhibitors to avoid the formation of gas hydrates. In 1944, Professor Katz and students at the University of Michigan made the first correlations for hydrate phase equilibria, saving time and money for industry by providing acceptable predictions [6]. In the late 1940s, Stackelberg and Müller determined via x-ray spectroscopy two hydrate crystal structures, SI and SII [7, 8]. In 1987 the third structure, SH, was discovered by Ripmeester [1].

In 1957 Barrer and Stuart suggested a statistical thermodynamic method to determine gas hydrate properties [1]. Two years later, van der Waals and Platteeuw proposed this method, which is the basis of the currently used ones [9]. This method uses microscopic properties such as intermolecular potentials to calculate macroscopic properties such as temperature or pressure. In the

oncoming years, several authors and researchers added improvements and special considerations to this method [1].

1.2. RELEVANCE TOWARDS GAS HYDRATES

After Hammerschmidt's discovery and the regulation of water content in pipe lines, gas hydrate researches with an industrial approach have been seen during the years. The production and processing in unusual environments, such as Siberia, Alaska, the North Sea and in Deep Ocean drilling, often leads to problems like undesirable gas hydrate formation inside pipelines during natural gas transport. The best known accident caused by gas hydrate is the explosion of the Piper Alpha Nord Sea platform in 1988, where the formation of gas hydrate blocked a pipe line, causing a gas leakage which conducted to an explosion [10].

Subsea gas and oil production are moving to deeper waters, which are associated with higher pressures and lower temperatures, the perfect stability zone for hydrates. For those processes, traditional methods such as heating for preventing hydrate formation are highly unprofitable, thus industry is starting to use kinetic inhibitors for example ethylene glycol in many North Sea applications or other uncommon methods, leading to a continuous expanding of gas hydrates investigation and understanding [11].

But gas hydrates are not only problem carriers. An estimation of Klauda and Sandler in the year 2005 calculated a methane quantity between $4.4*10^{16}$ and $1.2*10^{17}$ m^3 in hydrate form [12], which, compared to $1.4*10^{14}$ m^3 of actual methane gas reservoirs, makes gas hydrate importance not only an industrial risk factor, but also a political and social issue due to the energy reserve potential for an oncoming future. Also, it has been calculated that around 150 m^3 of gas can be stored in 1 m^3 of hydrate. This ability could be used for logistic in gas transportation or solutions for greenhouse gases storing, such as CO_2 [11].

It has to be noticed, that a wrong use of this natural gas hydrate or uncontrolled gas storage could aggravate today's global warming [2].

Several studies have been made towards gas hydrate understanding and prediction. In 1960s, a large experiment at the Gubkin Petrochemical and Gas

Industry Institute in the USSR was made for the goal of using natural gas hydrates as an energy source. In this experiment the kinetics of hydrate formation and thermodynamics were studied [1]. In 1992, gas hydrate formation in drilling applications stimulated measurements of hydrate formation in oil-based and in water-based drilling fluids, leading to a prediction method. Kobayashi and coworkers have measured hydrate equilibria for its application in single phase pipelines in cold regions, such as North Slope in Alaska or subsea [1]. In Scotland, Danesh, Todd and coworkers studied the inhibition with methanol and mixed electrolyte solutions. They also performed the most comprehensive study of systems with heavy hydrocarbons produced or transported in the North Sea [1]. In Canada, Robinson has performed the most comprehensive measurements of aqueous phase concentrations of methanol and glycol needed to inhibit hydrate formation [1]. In Bishnoi's laboratory, hydrate formation under shutdown conditions was measured, also in gas and condensate pipelines [1]. Hydrate blockage formation was studied in the Werner-Bolley gas line [1].

1.3. OBJECTIVES

This Bachelor Thesis work is based on two facts:

- Gas hydrates present a limitation in some crucial operations, making their phase equilibria study of high importance for industrial process design.

- The use of inhibitors such as salts, glycols or alcohols affect the gas hydrate formation conditions, which can be used to move those conditions away from the process.

Because of the two mentioned points, the main objectives of this Bachelor Thesis are:

1. Study the prediction of gas hydrate formation between water and common industrial gases and how gas hydrates limit processes in industry.

2. Study how inhibitors affect the formation of gas hydrates and how this inhibition affects processes for their application in industry.

2. THEORETICAL BACKGROUND

Gas hydrates are included in the group of solids called clathrates, which according to IUPAC are "Inclusion compounds in which the guest molecule is in a cage formed by the host molecule or by a lattice of host molecules". In this case, the host water molecule component, in a crystalline cage form, contains the guest gas component. Gases likely to form hydrates are nitrogen, oxygen, carbon dioxide, hydrogen sulfide and alkanes such as methane and ethane [1, 2].

2.1. STRUCTURE

Three different structures have been identified for gas hydrates: I, II and H. Other structures are been recently studied, but information about those new types are not widely known.

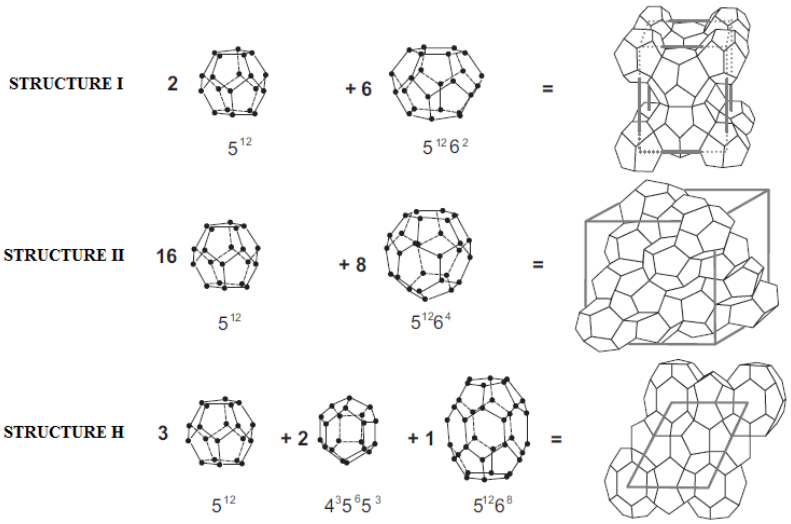

Figure 1: Spatial configuration of gas hydrate structures I, II and H [2].

Typical components forming structure I are carbon dioxide, methane or nitrogen and structure II is formed by gases like ethane and the binding components of structure I. The formation of structure H requires at least two different gases to exist, because the large cage can be stable only with large gases such as vanadyl sulfate and small gases help to stabilize the smaller cages [1].

Table 1: Crystallographic properties of hydrate structures I, II and H [2].

Structure	SI		SII		SH		
	Small	Big	Small	Big	Small	Middle	Big
Cage	5^{12}	$5^{12}6^2$	5^{12}	$5^{12}6^4$	5^{12}	$4^35^66^3$	$5^{12}6^8$
Cages per structure	2	6	16	8	3	2	1
Diameter (Å)	3.95	4.30	3.91	4.73	3.94	4.04	5.79
Coordination	Cubic Primitive		Cubic Face centered		Hexagonal		
Water molecules per str.	46		136		34		

2.2. PHASE BEHAVIOR

As in any other process, a question an engineer must ask himself is how many variables are needed for the phase equilibrium prediction, because in gas hydrates, not every possible hydrate behaves the same. For this problem, as in every other phase equilibrium calculation, the Gibb's Phase Rule is used, by means of the equation:

$$F = C - P + 2 \quad (1)$$

Where F is the number of intensive variables to specify, C is the number of components in the system and P is the number of phases [1, 3].

But after knowing the number of variables to be used, the engineer also has to know which variables he can use. The study of the phase equilibria is commonly ruled by temperature and pressure, concentrations, volume or density and phase amounts. Because temperature and pressure are easy to measure in processes, phase equilibrium can easily be predicted by these variables. On the other hand, variables like components density are difficult to measure, relegating them as equilibrium criteria. For concentration and phase amounts, the applicability is different.

Because of the difficulty of measuring with good reliability low concentrations of gases in the liquid phase or low concentrations of water in gaseous phases, the equilibrium must be explained with another variable easy to measure. The difficulty is not attributed to lack of equipment for this type of calculations. What occurs is

that normally engineers don't have in hand equipment such as dual chromatographic columns, NMR or Raman spectroscopy, which are available only in few laboratories. But engineers have access to equipment such as chromatographers which can measure water-free gaseous phase and gas-free liquid phase concentrations, making these two variables a criteria for phase equilibria analysis.

As a result, hydrate phase equilibria can be determined normally by four variables:

1. Temperature
2. Pressure
3. Water-free gas phase
4. Gas-free liquid phase.

With these variables, an engineer can specify the water-free gas composition and the gas-free liquid composition and can predict the hydrate formation temperatures for the process pressure, helping him guarantee protection against these undesirable formations.

2.3. PHASE EQUILIBRIA DIAGRAMS

The understanding of the hydrate phase-equilibria diagrams is supported by figure 2. The diagrams use symbols of I, L_W, H, V and L_{HC} to represent ice, liquid water, hydrate, vapor and liquid hydrocarbon. Systems are represented on a pressure-temperature diagram as an area (for two phases), a line (three phases) or a point (4 phases). To obtain straight lines, semi-logarithmic plots are used.

The first quadruple point (Q1) is where four phases coexist (I-L_W-H-V). The quadruple point temperature is the same for all hydrate formers, around 273K, but its pressure varies. The Q1 is the starting point of four equilibrium lines:

1. L_W-H-V is the line with most interest in natural gas systems.
2. I-H-V has a lower slope than the previous line.
3. I-L_W-H rises vertically from the quadruple point, showing large pressure changes for small temperature changes.

4. I-L_W-V connects the quadruple point to the water triple point, which is the transition from water to ice without hydrate formation.

   For systems which present only the Q1, the hydrate region is limited by the pressures and temperatures of the L_W-H-V and I-H-V lines. Only to the left of these lines hydrate can exist.

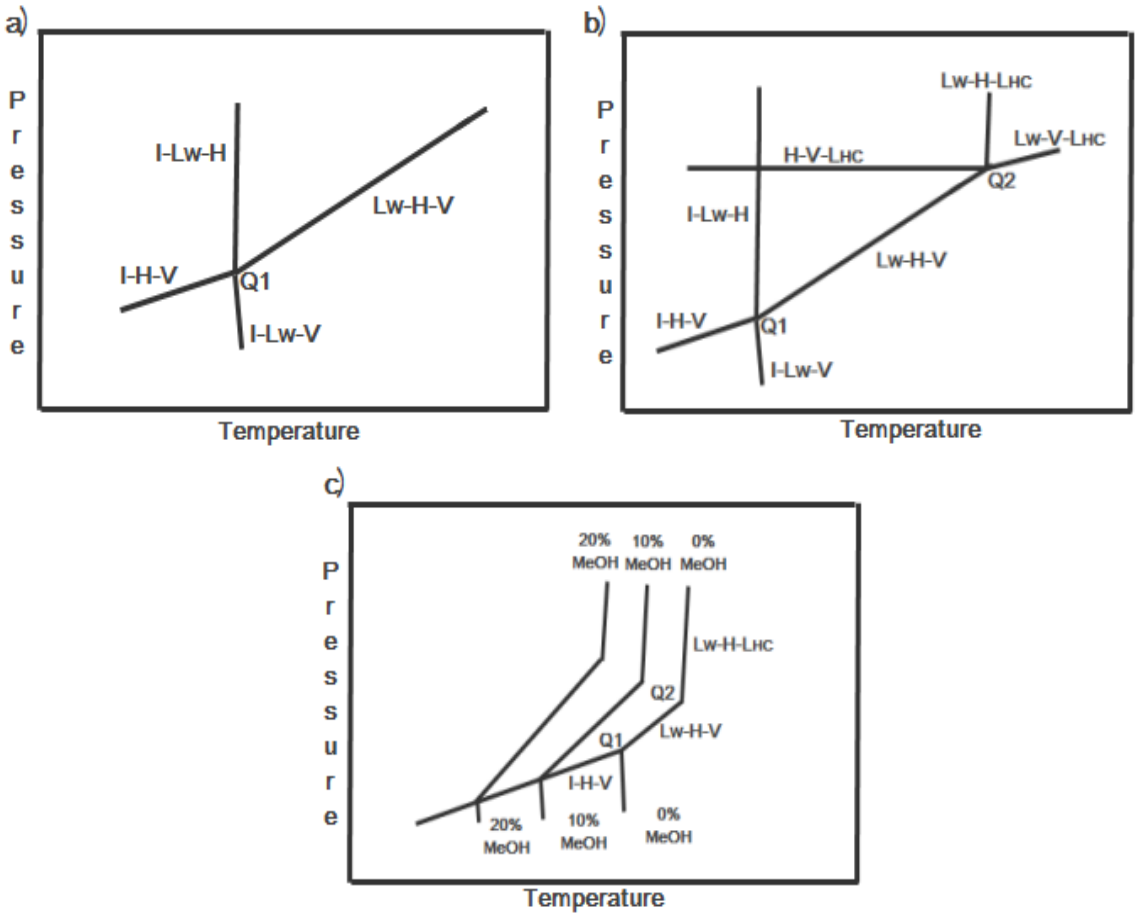

Figure 2: Pressure-temperature diagrams. a) Only Q1 system. b) Q2 system. c) Systems using inhibitors [1].

The intersection temperature of the Q1 closely approximates to the ice point, because the solubility of hydrate formers in water is normally too small to change the freezing point, even for carbon dioxide and hydrogen sulfide which present high solubility in water [1].

The second quadruple point (Q2), which is presented in more complex systems such as ethane + water, propane + water, carbon dioxide + water or hydrogen sulfide + water shows a new intersection where other four phases coexist (L_W-H-V-L_{HC}). Q2 is the starting point of three new equilibrium lines:

1. L_W-V- L_{HC}, this line is similar to the vapor pressure line of the pure hydrocarbon.
2. L_W-H- L_{HC}, highly vertical line due to incompressibility of the gases in the phase.
3. H-V-L_{HC}, this line has not great concern, because it exists inside the boundaries of L_W-H- L_{HC} and L_W-H-V.

For systems which present Q2, the hydrate region is bounded by line I-H-V at conditions below the Q1, line L_W-H-V between Q1 and Q2 and line L_W-H- L_{HC} at conditions above Q2. To the left of these lines hydrate formation is possible and not to the right. Q2 is often approximated as the maximum temperature of hydrate formation, because the vertical slope of the line L_W-H- L_{HC}.

The temperature and pressure of Q2 is provided by the intersection between L_W-H-V line and the pure component vapor pressure line. The pure component is taken as a good approximation, due to the highly low vapor pressure that water presents and the almost complete immiscibility between water and the liquid component at these conditions [1].

2.3.1. ONLY Q1 SYSTEMS

The most typical component that make part of these systems is methane, the liquid hydrocarbon phase doesn't exist, making lines with L_{HC} impossible and thus no Q2 if found. Also, in this type of system, the L_W-H-V line has no upper pressure or temperature limit, due to the low critical temperatures they present. It means that the critical points are far away from Q1, preventing an intersection of the vapor pressure line with the L_W-H-V line. In the line I-L_W-H has been found that an upper pressure doesn't exist. Also, in this same line is observed large pressure changes by small temperature changes, attributed to an incompressible phase.

In this equilibrium plots, three two-phase regions are described between two equilibrium lines. Between the lines L_W-H-V and I-H-V is the H-V region in which

hydrates are in equilibrium only with vapor. The L_W-H region exists between L_W-H-V and I-L_W-H lines and the I-H region exists between I-L_W-H and I-H-V [1].

2.3.2. SYSTEMS PRESENTING Q1 AND Q2

In these types of systems, components like ethane, propane, isobutene, carbon dioxide or hydrogen sulfide are found, which are components capable of presenting a L_{HW} region similar to the pure component vapor pressure line.

In these systems two two-phase region are described between three equilibrium lines. Between the lines I-L_W-H, L_W-H-V and L_W-H- L_{HC} the region L_W-H exists and the H-V region exists between H-V-L_{HC}, L_W-H-V and I-H-V. Also, two two-phase regions are described between two equilibrium lines. The region I-H exists between I-L_W-H and I-H-V and the new region H- L_{HC} is between L_W-H- L_{HC} and H-V-L_{HC} [1].

2.3.3. INHIBITED SYSTEMS

As mentioned before, conventional methods are not profitable for companies and for example in gas transport pipe lines a method such as heating would be impossible to achieve. Thus, new methods for hydrate prevention have been studied. Inhibited systems using alcohols, glycols or salts have gained great attention and nowadays there is considerable information about them. Other inhibitors have been tried, but less successful as the before mentioned. Using ammonia in a carbon dioxide hydrate system causes for example an undesirable reaction, forming ammonium carbonate and ammonium carbamate, which are more difficult to remove than hydrates.

In general terms, the inhibition takes place due to the competition for the water molecules between the inhibitor and the gas, by means of hydrogen bonding for alcohols and glycols or coulombic forces with salts. As for pure water, adding a solute to the system will cause a temperature depression effect, in this case to the hydrate formation temperature, as seen in figure 2. Nielsen and Bucklin [1] studied this effect and observed that this temperature depression will always be less than the ice depression temperature, by a factor equal to the heat of fusion of ice

divided by the heat of hydrate dissociation, with a numerical value between 0.6 and 0.7.

By Gibbs's Rule, explained before, adding a new component makes indispensable to have information about a new intensive variable. For this, the concentration of the inhibitor in the free-gas liquid phase is used [1].

2.3.3.1. ALCOHOL AND GLYCOLS

All alcohols and glycols form hydrogen bonds to water with their hydroxyl group. Additionally it has been studied that the hydrocarbon end of the alcohol molecule causes a clustering effect on water molecules similar to hydrate formers. These two effects are in direct competition with the hydrate formers effects.

Of alcohols, methanol has been the most popular inhibitor, due to its cost and effectiveness, as indicated by Katz et al. [1] the inhibition ability increases with volatility. Methanol is used through gas injection in pipe lines, however, the use of methanol has become expensive, so methanol recovery and return lines are becoming more common, but its recovery is not very effective.

On the other hand, glycols such as ethylene glycol (EG), diethylene glycol (DEG) and triethylene glycol (TEG), provide more hydrogen bonding opportunity with water, because the extra hydroxyl groups they present, as well as the oxygen atoms in the case of larger glycols. Also, the glycols generally have higher molecular weights with lower volatility, so they can be recovered and recycled easier than alcohols, precisely than methanol [1].

2.3.3.2. SALTS

The action of salts as inhibitors differs from alcohols and glycols. In this case, salts dissociate in solution and interact with the dipoles of water with coulombic bonds, which are stronger than either the hydrogen bond or the clustering effect caused by the hydrocarbon part of alcohols and glycols. The stronger bonds of water with salt ions inhibit takes place because water is more attracted to ions than to forming hydrate structures with gases.

A second effect has been studied, the so call “salting out”, where the solubility of potential hydrate guest molecules decreases. This two combined effects depress highly hydrate forming temperature, requiring more sub cooling for it to occur.

Industrially, alcohols and glycols are better solutions, because the risk of corrosion inside pipe due to salts [1].

3. THERMODYNAMIC BACKGROUND

As described in the gas hydrate history, the statistical thermodynamic model suggested by Barrer and Stuart [1] and developed by van der Waals and Platteeuw [9] is the basis for the gas hydrate equilibria prediction; and is the theoretical background for the HYCAL computer program developed by Rock [3] and improved by Windmeier [2] for the prediction of gas hydrate formation, with the difference in chemical potential as iteration parameter [1].

For the calculation of the chemical potentials, the gas components fugacity coefficients and the water activity coefficient need to be calculated through the use of thermodynamic models. The models that will be discussed are the ones which are going to be used for the calculations. These are:

1. Predictive Soave-Redlich-Kwong (PSRK) [19].
2. Volume Translation Peng-Robinson (VTPR) [34].
3. PSRK linked to the group contribution model LIFAC (PSRKLIFAC), when electrolytes are in the system [16].

3.1. THE STATISTICAL THERMODYNAMIC MODEL FOR HYDRATE EQUILIBRIA CALCULATION

The statistical thermodynamic model for hydrate equilibria calculation is based on the following theories:

1. Grand canonical partition function for water.
2. The chemical potential of water in hydrates.
3. The Langmuir adsorption analogy.
4. Relating the Langmuir constant to parameters.

But before these theories can be explained, four fundamental assumptions based upon structure were done by Waals and Platteeuw [9]:

- The host molecule’s contribution to the free energy is independent of the occupation of the cavity. This also implies that encaged molecules don’t distort the cavity.
- Each cavity can contain at most one guest molecule.

- There are no interactions between the guest molecules. It means that the energy of each guest molecule is independent of the number and types of other guests.
- No quantum effects are need; classical statistics are valid [1].

3.1.1. GRAND CANONICAL PARTITION FUNCTION FOR WATER AND THE CHEMICAL POTENTIAL OF WATER IN HYDRATES.

With these assumptions and with the grand canonical partition function as starting point, the simplified and final form of the grand canonical partition function for water is:

$$E = e^{\frac{-A^{\beta}}{kT}} * \prod_J \left(1 + \sum_i q_{J,i} * \lambda_J\right) \quad (2)$$

Relating the grand canonical partition function to macroscopic properties results into:

$$k * T * d\ln E = (-\mathrm{k} * \ln E + S)dT + PdV + \sum_J k * T * N_J * d\ln E * \lambda_J - \mu_W^H * dN_W \quad (3)$$

By differentiating $ln\,E$ with respect to the absolute cavity (λ) of *J*, provides the total number of gest molecules *J* over all the cavities *i*, as next:

$$N_{J,i} = \frac{v_i * N_W * q_{J,i} * \lambda_J}{(1 + \sum_J q_{J,i} * \lambda_J)} \quad (4)$$

Equation 4 can be used to determine the simple probability $\theta_{J,i}$ of finding a molecule of type *J* in a cavity of type *i*. This value is obtained by dividing $N_{J,i}$ by the total number of cavities *i* ($v_i * N_W$)

$$\theta_{J,i} = \frac{q_{J,i} * \lambda_J}{1 + \sum_J q_{J,i} * \lambda_J} \quad (5)$$

Equation 3 also allows calculating the chemical potential of the host μ_W^H as:

$$\frac{\mu_W^H}{k*T} = \frac{\mu_W^{\beta}}{k*T} - \sum_i v_i * \ln\left(1 + \sum_J q_{J,i} * \lambda_J\right) \quad (6)$$

Equation 5 may be simplified by relating $q_{J,i}$ and λ_J through a constant $C_{J,i}$, defined as:

$$C_{J,i} \equiv \frac{q_{J,i}*\lambda_J}{P_J} \quad (7)$$

So equation 5 results into the equation for the fractional occupation, as follows:

$$\theta_{J,i} = \frac{C_{J,i}* P_J}{1+\sum_J C_{J,i}* P_J} \quad (8)$$

Equation 8, also called Langmuir isotherm, can be considered as elementary probability of cavity *i* occupation by molecule *J*, where the coefficient $C_{J,i}$ depends of the temperature value and the type of cage.

When the fluid in equilibrium with the hydrate is non ideal gas, the pressure of component *J* is changed to its fugacity, as:

$$\theta_{J,i} = \frac{C_{J,i}* f_J}{1+\sum_J C_{J,i}* f_J} \quad (9)$$

Using equation 6 and relating the terms $q_{J,i}\ and\ \lambda_J$ to the constant $C_{J,i} * P_J$, is obtained:

$$\frac{\mu_W^H}{k*T} = \frac{\mu_W^\beta}{k*T} - \sum_i v_i * \ln\left(1 + \sum_J C_{J,i} * P_J\right) \quad (10)$$

A relation between equation 9 and the logarithmic term of equation 10 is done as follows:

$$\ln(1 - \sum_J \theta_{J,i}) = \ln\left(1 - \frac{C_{J,i}* P_J}{1+\sum_J C_{J,i}* P_J}\right) = \ln\left(\frac{1}{1+\sum_J C_{J,i}* P_J}\right) = -\ln\left(1 + \sum_J C_{J,i} * P_J\right)$$

The same as:

$$\ln\left(1 + \sum_J C_{J,i} * P_J\right) = -\ln(1 - \sum_J \theta_{J,i}) \quad (11)$$

Substituting equation 11 with equation 10, the function for the calculating the chemical potential of water in hydrate is obtained:

$$\mu_W^H = \mu_W^\beta + k * T * \sum_J v_I * \ln\left(1 - \sum_J \theta_{J,i}\right) \quad (12)$$

Equation 12 is one of the major contributions of the statistical thermodynamics model. The combination of this equation and occupancy grade equation is of vital

importance to phase equilibrium calculations, at constant pressure and temperature.

Where the term:

$$k * T * \sum_J v_I * \ln\left(1 - \sum_J \theta_{J,i}\right) \quad (13)$$

Is also denoted $\Delta\mu_W^{\beta-H}$, the difference of water chemical potential between empty hydrate and occupied hydrate form, it means, it is the chemical potential of the stored gas component.

For the study of gas hydrates, the difference of the chemical potential between water in hydrate and empty hydrate form has to be known to allow the prediction of phase equilibria. This is because depending on its value the water is more likely to be in hydrate form or stay in its normal form (liquid (L) or ice(α)). The equation that relates this chemical potential is:

$$\Delta\mu_W^{H-L} = \Delta\mu_W^{\beta-L} + R * T * \ln(a_w) \quad (14)$$

If water is in ice phase, the term $\ln(a_w)$ is 1, giving:

$$\Delta\mu_W^{H-\alpha} = \Delta\mu_W^{\beta-L} \quad (15)$$

For the calculation of $\Delta\mu_W^{\beta-L}$, the following equation is derived:

$$\frac{\Delta\mu_{0W}^{\beta-L}(\mathrm{T,p})}{R*T} = \frac{\Delta\mu_{0W,0}^{\beta-L}(\mathrm{T_0,p_0})}{\mathrm{R*T_0}} - \int_{\mathrm{T_0}}^{\mathrm{T}} \frac{\Delta h_{0W}^{\beta-L}(\mathrm{T,p_0})}{R*T^2} dt + \int_{\mathrm{p_0}}^{\mathrm{p}} \frac{\Delta v_{0W}^{\beta-L}(\mathrm{T_0,p})}{R*T^2} dp \quad (16)$$

All the delta values at standard conditions needed are already calculated, they depend only on the type of structure, not on the type of cage or component [1-3].

3.1.2. THE LANGMUIR ADSORPTION ANALOGY

Sloan and Koh [1], made an easy explanation of this analogy as follow:

Single component Langmuir adsorption isotherm assumptions are:

- The adsorption of gas molecules occurs at discrete sites on the surface.
- The energy of adsorption on the surface is independent of the presence of other adsorbed molecules.
- The maximum amount of adsorption corresponds to one molecule per site.

- The adsorption is localized and occurs by collision of gas phase molecules with vacant sites.
- The desorption rate depends only on the amount of adsorbed material on the surface

And if we replace the words “adsorption or desorption” to “enclathration or declathration” the word “sites” by “cavities” and the word “surface” by “crystal unit cell”, we obtain the analogy for gas hydrates.

Also, this analogy can be seen from the Langmuir adsorption isotherm equation:

$$\theta = \frac{K*P_J}{1+ K*P_J} \tag{17}$$

Comparing Langmuir adsorption isotherm equation with equation 8 shows that both equations are almost the same. The Langmuir hydrate constant $C_{J,i}$ is analogous to the Langmuir constant K and both equations are function of temperature and the type components. The only difference is that Langmuir constant in hydrates also depends of the type of cavity, providing an additional subscript i and a summation of terms in the denominator.

Additionally, taking into account the two types of cages that structures SI and SII present, the equation is expanded as follows:

$$\theta_{j,i}{}^{k} = \frac{{C_{j,i}}^{k}*f_j^k}{1+\sum_k\sum_J {C_{j,i}}^{k}*f_j^k} \tag{18}$$

For this last equation 3 different possibilities of filling can be possible:

- Empty cage, having:

$$\theta_{j,i}{}^{k} = \frac{1}{1+\sum_J {C_{j,i}}^{1}*f_j+ {C_{j,i}}^{2}*f_j} \tag{19}$$

- Single caging, having:

$$\theta_{j,i}{}^{k} = \frac{{C_{j,i}}^{1}*f_j}{1+\sum_J {C_{j,i}}^{1}*f_j+ {C_{j,i}}^{2}*f_j} \tag{20}$$

- double caging, having:

$$\theta_{j,i}{}^{k} = \frac{{C_{j,i}}^{2} * f_j^2}{1 + \sum_J {C_{j,i}}^{1} * f_j + {C_{j,i}}^{2} * f_j} \quad (21)$$

For the use of these equations, Langmuir constants have to be predicted. For this, the Langmuir constants $C_{J,i}$ can be related to experimental variables, as describe in the next section [1-3].

3.1.3. RELATING THE LANGMUIR CONSTANT

3.1.3.1 KIHARA POTENTIAL PARAMETER

In 1963, McKoy and Sinanoglu suggested the Kihara Potential Parameter model [1], with parameters fitted to experimental hydrate dissociation data. This model is currently used, however the equations presented next are for a spherical core; non spherical core works has not been done for hydrates.

Before relating it with the Langmuir constants, two extra assumptions have to be made in addition to the four at the beginning of section 3.1 which are:

- The internal motion partition function of the guest molecule is the same as that of an ideal gas. It means that the rotational, vibrational, nuclear and electronic energies are not significantly affected by enclathration.
- The potential energy of a guest molecule at a distance r from the cavity center is given by the spherically symmetrical potential ω(r).

The Kihara Potential Parameter model obtains a function ω(r) describing the resulting field, averaged over all positions of the molecules within the cavity. The fundamental intermolecular potential between the water molecule of the cavity wall and a solute molecule may be described by a number of intermolecular potentials.

The pair potential energy φ is itself a function of the separation distance, (r) between the guest molecule and any water molecule, also called molecular center distance. The function is given by:

$$\Phi(\mathrm{r}) = \infty \qquad for\ r\ \leq (a_g + a_w) \quad (22)$$

$$\Phi(\mathrm{r}) = 4 * \varepsilon * \left\{ \left(\frac{\sigma}{r - 2 * a} \right)^{12} - \left(\frac{\sigma}{r - 2 * a} \right)^{6} \right\} \quad for\ r\ > (a_g + a_w) \quad (23)$$

The Leonard-Jones-Devonshire theory [1] averaged the pair potentials of equations 22 and 23 between the solute and each water molecule, to obtain the cell potential function ω(r):

$$\omega(\mathrm{r}) = 2 * z * \varepsilon * \left\{\frac{\sigma^{12}}{R^{11} * r} * \left(\delta^{10} + \frac{a}{R} * \delta^{11}\right) - \frac{\sigma^{6}}{R^{5} * r} * \left(\delta^{4} + \frac{a}{R} * \delta^{5}\right)\right\} \quad (24)$$

Where

$$\delta^{N} = \frac{1}{N} * \left\{\left(1 - \frac{r}{R} - \frac{a}{R}\right)^{-N} - \left(1 + \frac{r}{R} - \frac{a}{R}\right)^{-N}\right\} \quad (25)$$

The parameters ε, a and σ are unique for every guest molecule, but they do not change in the different cavities. On the other hand, the parameters z and R are unique for each type of cavity and do not depend of the molecule.

A typical potential $\omega(\mathrm{r})$ shown in figure 3, notes that the potential is more negative (more attraction) in the center of the cell, or at some distance from the cell wall, with high repulsion (positive values) at the cell wall. As the guest molecule approaches one wall of the cavity, it is both repulsed by the wall and attracted by the opposite, causing it to exist in the center.

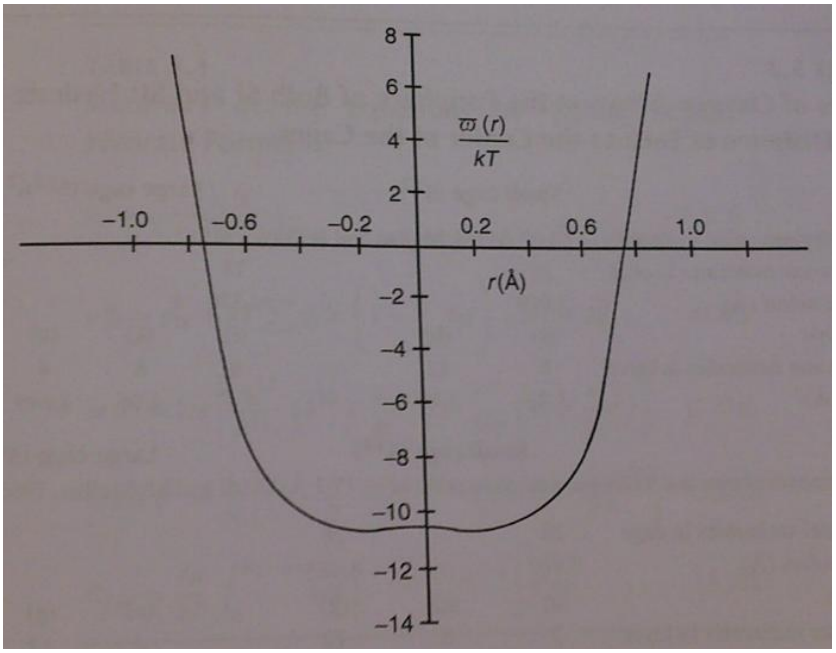

Figure 3: Typical spherically symmetrical cavity potential function between guest and cell [1].

The final expression for the Langmuir constant in terms of the particle potential within the whole cavity results as:

$$C_{J,i} = \frac{4*\pi}{k*T} * \int_0^R e^{\left(-\frac{\omega(r)}{k*T}\right)} * r^2 * dr \quad (26)$$

Equation 26 provides the evaluation of the Langmuir constant from a minimum of experimentally fitted Kihara parameters via an integration over the cavity radius, also it is seen that the constant is only a function of temperature for a given component within a given cavity [1-3].

3.1.3.2. OTHER EXPERIMENTAL FITTED PARAMETERS

In the Ph.D. work from Windmeier [2], a new function for the calculation of the Langmuir constant is shown, called Integral Central Well Potential model:

$$C_{J,1}^{(1)} = C_{J,1}^{(1),0} * e^{\left(-\frac{\varepsilon_{J,1}^1}{R*T}\right)} \text{ for SI} \quad (27)$$

$$C_{J,1}^{(2)} = C_{J,1}^{(2),0} * e^{\left(-\frac{\varepsilon_{J,2}^2}{R*T}\right)} \text{ for SII} \quad (28)$$

These fitted parameters model reduce mathematical calculations, since no numerical methods need to be used for calculations, like for the integral in equation 26.

Since there are only eight simple hydrate formers of natural gas, but infinite possibilities of combinations, fitting experimental hydrate formation data for the calculation of Langmuir constants help to a good prediction of hydrate formation, representing time and effort saving on the research of each type of combination [1, 2].

3.2. FUGACITY AND WATER ACTIVITY COEFICIENT CALCULATIONS

As mentioned on the beginning of chapter 3 and described in the hydrate models equations, fugacity coefficients and activity coefficients are needed for the prediction. Because of this, thermodynamic models such as equations of state or group contribution methods are used.

3.2.1. EQUATIONS OF STATE (EOS)

The van der Waals equation of state (Eq. (29)) was the first cubic equation of state ever introduced for the calculation of PVT systems [31]. With this equation effects like evaporation, critical phenomenons and condensation or multiphase equilibria could be described.

$$P = \frac{R*T}{v-b} - \frac{a}{v^2} \tag{29}$$

Although this model was one of the most important developments in thermodynamics, it presents many disadvantages like poor results in the calculation of liquid densities and vapor pressures. To improve these results, many other authors have presented a large number of modified equations of state.

One example is the Soave-Redlich-Kwong (SRK) equation of state [32]:

$$P = \frac{R*T}{v-b} - \frac{a(T)}{v*(v+b)} \tag{30}$$

In this equation a temperature dependent attractive parameter $a(T)$ was introduced, with it great improvements in the calculation of vapor pressures were achieved. Soave introduced the temperature dependence of the *a* parameter with the help of the α -function:

$$\alpha_{ii}(T) = \left[1 + (0.48 + 1.574 * \omega_i - 0.176 * \omega_i^2) * \left(1 - T_{r,i}^{0.5}\right)\right]^2 \tag{31}$$

Another example is the Peng-Robinson (PR) equation of state (Eq. (32)) [33], where an improvement for the prediction of liquid densities by suggesting a different model was done, also a modified α –function is presented (Eq. (33)).

$$P = \frac{R*T}{v-b} - \frac{a(T)}{v*(v+b)+b*(v-b)} \tag{32}$$

$$\alpha_{ii}(T) = \left[1 + (0.37464 + 1.54226 * \omega_i - 0.26992 * \omega_i^2) * \left(1 - T_{r,i}^{0.5}\right)\right]^2 \tag{33}$$

For mixtures, the calculation of the attractive parameter a and the co-volume parameter b are done by the use of mixing rules (Eq. (35, 36)), also the parameter ***a*** in the EOS changes to a_m and ***b*** changes to b_m, as for example the PR EOS results:

$$P = \frac{R*T}{v-b_m} - \frac{a_m}{v*(v+b_m)+b_m*(v-b_m)} \quad (34)$$

At the beginning, the application of the equations of state for mixtures was done using the classical van der Vaals mixing rule, which were limited to non-polar or slightly polar systems.

$$a_m = \sum\sum x_i x_j a_{ij} \quad (35)$$

$$b_m = \sum\sum x_i x_j b_{ij} \quad (36)$$

The combining rules for a_{ij} and b_{ij} are:

$$a_{ij} = \sqrt{a_i a_j} * \left(1 - \alpha_{ij}\right) \quad (37)$$

$$b_{ij} = \sqrt{b_i b_j} * \left(1 - \beta_{ij}\right) \quad (38)$$

Where the parameters α_{ij} and β_{ij} are calculated by regression analysis of experimental phase equilibrium data [35].

3.2.2. GROUP CONTRIBUTION METHODS

For the aim of this work the liquid water activity coefficient is needed, as seen in equation 14. For this, the g^E mixing rule EOS already mentioned at the beginning of the section are used, which are based on the group contribution methods UNIFAC and LIFAC.

These group contribution methods are based on the solution of group concept [14], which states that the functional groups of the chemical components are always the same in many different molecules. The majority of chemical compounds are constituted by carbon, hydrogen, oxygen, nitrogen, halogens, sulfur, phosphorous and other more, which combined make the functional groups

used for the prediction on this method. The advantage of dividing the structures into functional groups is that their number is much smaller than the number of possible compounds; this means that with a limited number of functional groups, the behavior of a large number of systems can be predicted [14].

For the prediction of mixture properties, except alkane-alkane mixtures, group interaction parameters fitted to a comprehensive database of binary experimental data are required. Common sources for these parameters are data banks like the DDB.

3.2.2.1 UNIFAC

In this model, the activity coefficient γ_i is calculated by:

$$\ln \gamma_i = ln\, \gamma_i^C + \ln \gamma_i^R \qquad (39)$$

Where the combinatorial part $\ln \gamma_i^C$ takes into account the size and form of the molecules and the residual part $\ln \gamma_i^R$ deals with the interactions between the various groups. γ_i is obtained from the group activity coefficients in the mixture Γ_k and in the pure component i ($\Gamma_k^{(i)}$) following Eq. (40):

$$\ln \gamma_i^R = \sum v_k^{(i)} * \left(\ln \Gamma_k + \ln \Gamma_k^{(i)}\right) \qquad (40)$$

But this method shows weakness for the calculation of activity coefficients at infinite dilution, excess enthalpies and asymmetric systems. To eliminate those problems, a modified UNIFAC Dortmund was developed [15]. In this method, the combinatorial part changes, new groups are defined and temperature dependent group interaction parameters were introduced.

3.2.2.2 LIFAC

For the calculation of the water γ_i for systems containing electrolytes, the group contribution method LIFAC can be used. It provides reliable calculation of the liquid γ_i up to high salt concentrations for the different ions and solvents. The function for the activity coefficient is:

$$\ln \gamma_i = \ln\gamma_i^{LR} + \ln \gamma_i^{MR} + \ln\gamma_i^{SR} \quad (41)$$

The first term $\ln\gamma_i^{LR}$ represents the long-range (LR) interaction contribution caused by the charge-charge interactions, parameters that are found in the LIFAC matrix of interactions.

The second term $\ln \gamma_i^{MR}$ represents the Middle-range (MR) interactions caused by charge dipole and charge induced dipole interactions. These parameters are already published.

The third parameter $\ln\gamma_i^{SR}$ represents the short-range (SR) interactions caused by the non-charged interactions, similar to SR interactions in nonelectrolyte solutions, which can be taken from the PSRK interaction parameters matrix [16].

3.2.3. g^E MIXING RULE

Huron and Vidal [17] combined the advantages of the g^E models and the EOS by the development of a g^E mixing rule at a reference pressure $P^{ref} = \infty$:

$$\frac{a}{b*R*T} = \sum_i x_i * \frac{a_{ii}}{b_i*R*T} + \frac{g_\infty^E/_{RT}}{-0.6931} \quad (42)$$

Great improvements were obtained with this rule; while for the SRK equation of state in combination with the classical quadratic mixing very poor results were obtained for polar systems, the vapor liquid equilibria of these systems can be described accurately by using a g^E mixing rule [13].

Michelsen [18] derived a first order modified Huron Vidal mixing rule at a reference pressure of 0 bar:

$$q_1 * \left(\frac{a}{b*R*T} - \sum_i x_i * \frac{a_{ii}}{b_i*R*T}\right) = \frac{g_0^E}{RT} + \sum_i x_i * \ln\frac{b}{b_i} \quad (43)$$

With q1 depending on the type of EOS used.

The next three g^E mixing rule EOS are the ones which are going to be used in the predictive computational tool for the calculations of gas components fugacity and water activity coefficient.

3.2.3.1 PREDICTIVE SOAVE-REDLICH-KWONG (PSRK)

This method is the combination of the SRK equation of state and the g^E model UNIFAC, published in 1991 by Holderbaum and Gmehling [19]. The PSRK - g^E mixing rule for the parameters a at a reference state of P^{ref} = 1.01325 bar is:

$$\frac{a}{b*R*T} = \sum_i x_i * \frac{a_{ii}}{b_i*R*T} + \frac{{}^{g_0^E}/_{RT} + \sum_i x_i * \ln {}^{b}/_{b_i}}{0.64663} \quad (44)$$

Where the values of a_{ii} are functions of $\alpha_{ii}(T)$, b_i function of the component properties and the parameter b is calculated using the classical linear mixing rule.

The α - function used, is the one proposed by Mathias and Copeman [20], which is for $T_r < 1$:

$$\alpha_{ii}(T) = \left[1 + c1 * \left(1 - T_{r,i}^{0.5}\right) + c2 * \left(1 - T_{r,i}^{0.5}\right)^2 + c3 * \left(1 - T_{r,i}^{0.5}\right)^3\right]^2 \quad (45)$$

For $T_r > 1$, the parameters $c2$ and $c3$ are equal to zero, leading to:

$$\alpha_{ii}(T) = \left[1 + c1 * \left(1 - T_{r,i}^{0.5}\right)\right]^2 \quad (46)$$

3.2.3.2. PSRK-LIFAC

This model is an extension of the PSRK model for systems containing strong electrolytes. For the liquid phase, the g_0^E can be calculated as:

$$g_0^E = R * T * \sum_i x_i' * \ln \gamma_i' \quad (47)$$

Where x_i' is the salt-free mole fraction in the liquid phase, and γ_i' is the activity coefficient on a salt-free basis of component i, which this last is calculated as:

$$\gamma_i' = \sum_s x_s * \gamma_i \quad (48)$$

Where s counts for all the electrolytes and γ_i is calculated using the LIFAC model of section 3.2.2.2.

Combining Eq. 47 and 48 with the PSRK - g^E mixing rule (Eq. (44)), the PSRK-LIFAC - g^E mixing rule is obtained:

$$\frac{a}{b*R*T} = \sum_i x_i * \frac{a_{ii}}{b_i*R*T} + \frac{\sum_i x_i' * \ln(\sum_s x_s * \gamma_i) + \sum_i x_i * \ln^b/_{b_i}}{0.64663} \quad (49)$$

For the b parameter the classical linear mixing rule is used, with x_i' instead of x_i as follows [16]:

$$b = \sum\sum x_i' x_j' b_{ij} \quad (50)$$

3.2.3.3. VOLUME TRANSLATED PENG-ROBINSON (VTPR)

The VTPR [34] model is based on the PR equation of state and the group contribution method modified UNIFAC Dortmund [26]. Also, modern mixing rules for the parameters a and b suggested by Chen et al. [24] are used.

To improve the prediction for liquid densities, the concept of volume translation proposed by Peneloux et al. [23] was introduced. The component specific translation parameter c_i is obtained as a difference between PR EOS calculated volumes and experimental volumes at a reduced temperature of 0.7 (Eq. (52)).

$$c_i = v_{i,PR} - v_{i,exp} \quad (51)$$

For mixtures, the translation parameter c can be calculated following the linear mixing rule shown in Eq. 52.

$$c = \sum_i x_i * c_i \quad (52)$$

The VTPR model function is:

$$P = \frac{R*T}{v+c-b} - \frac{a(T)}{(v+c)*(v+c+b)+b*(v+c-b)} \quad (53)$$

For the calculation of $a(T)$, the Twu α - function [20] is used.

$$\alpha_{ii}(T) = T_{r,i}^{N_i*(M_i-1)} e^{\left[L_i*\left(1-T_{r,i}^{N_i*M_i}\right)\right]} \quad (54)$$

Also a change in the g^E mixing rule is presented, referenced at 1.01325 bar:

$$\frac{a}{b} = \sum_i x_i * \frac{a_{ii}}{b_{ii}} + \frac{g_{ref}^E}{-0.53087} \quad (55)$$

With the parameter b calculated using the following quadratic mixing rule:

$$b = \sum_i \sum_j x_i * x_j * b_{ij} \quad (56)$$

Where b_{ij} is derived from a non-linear combination rule with ¾ as exponent adopted from mod. UNIFAC (Do) [13]:

$$b_{ij} = \frac{b_{ij}^{3/4} + b_{ij}^{3/4}}{2} \quad (57)$$

4. COMPUTATION

After all the models for the prediction of hydrates were done, many authors have realized computational programs for the prediction of hydrate phase equilibria. For example CSMGem from Colorado School of Mines in the year 2007, CSMHYD from the same school but in 1998, DBRHydrate from DBRobinson Software Inc., Multiflash from Infochem Computer Services Ltd. and more others [1].

An available computer algorithm from a software called HYCAL, developed by Rock in 2002 in FORTRAN language [2] and improved by Windmeier in 2009 [3], provides a calculation of the gas hydrate phase equilibria and was the base tool for the development on this thesis work. On it three different methods are provided:

1. TV: Calculating equilibrium temperature for a given pressure and constant gas composition.
2. TP: Calculating equilibrium pressure for a given temperature and constant gas composition.
3. PY: Calculating equilibrium pressure for a given temperature and moving gas composition.

The most important difference that Windmeier's routine presents in comparison with Rock's is that Windmeier suggests and presents a different model for the Langmuir constants calculation, the Integral Central Well Potential model.

Windmeier's routine can be seen in figure 4, this routine is the one which is going to be used for the present work. For calculations of fugacity of gases and activity of water, HYCAL uses models such as SRK, UNIQUAC combined with SRK or PITZER for systems where salts are used.

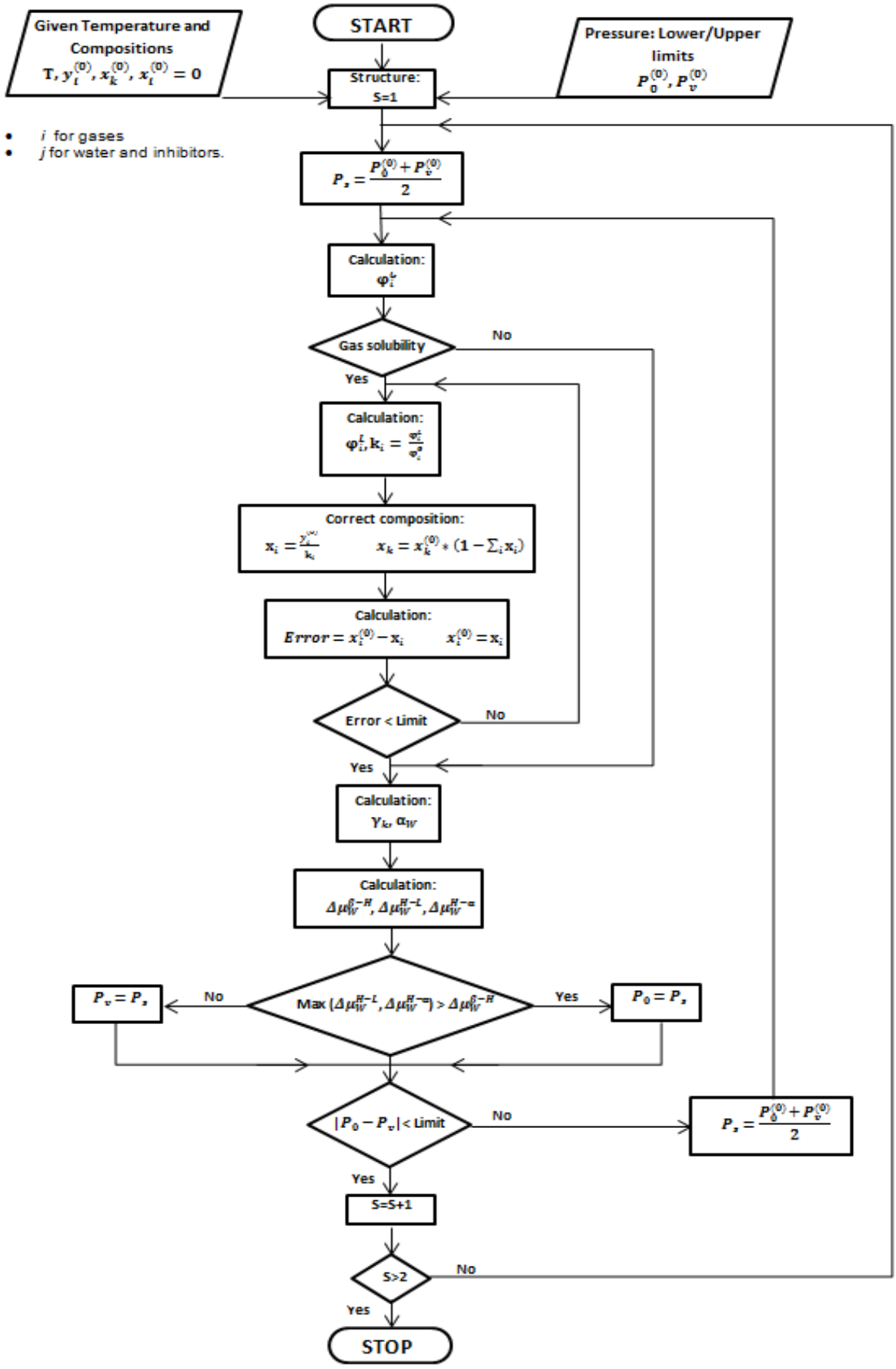

Figure 4: TP routine developed by Windmeier.

4.1. IMPROVEMENT OF PERFORMANCE

Thermodynamic models used by Windmeier in HYCAL for fugacity and water activity coefficients could be enhanced or changed to get better precision in the prediction calculations. Also, more models could be added to have more options for prediction, due to the fact that not every model behaves equally for every component or mix of components.

Predictive models from DDB were used, which have been developed since many years and present high accurate results. The models which were used are the ones explained in the previous section 3.2.3.

Besides more accurate and strong thermodynamic models, HYCAL was improved by adding more features to a new implementation, like a user interface for easy data input and output, with different possibilities for the last one, like automatic plots and tabled data. Also, more inhibitors components can be used from DDB, giving the possibility to predict more systems.

For the new implementation, the code was written from FORTRAN language to C++, because of the next reasons:

- To add more models or functions to FORTRAN code is a hard task, since many changes have to be made internally.
- The input and output of HYCAL is not comfortable for a common user.
- C++ gives the opportunity of making a user interface program, so data can be input easily and output data can be easy to handle or to plot.
- The DDB prediction models are already written in C++ language, so they can be called from a C++ implementation.
- DDB provides a great and large pure components data bank for all the needed properties.
- For model development also huge number of experimental data is needed, which can easily be taken from the DDB using existing infrastructure.

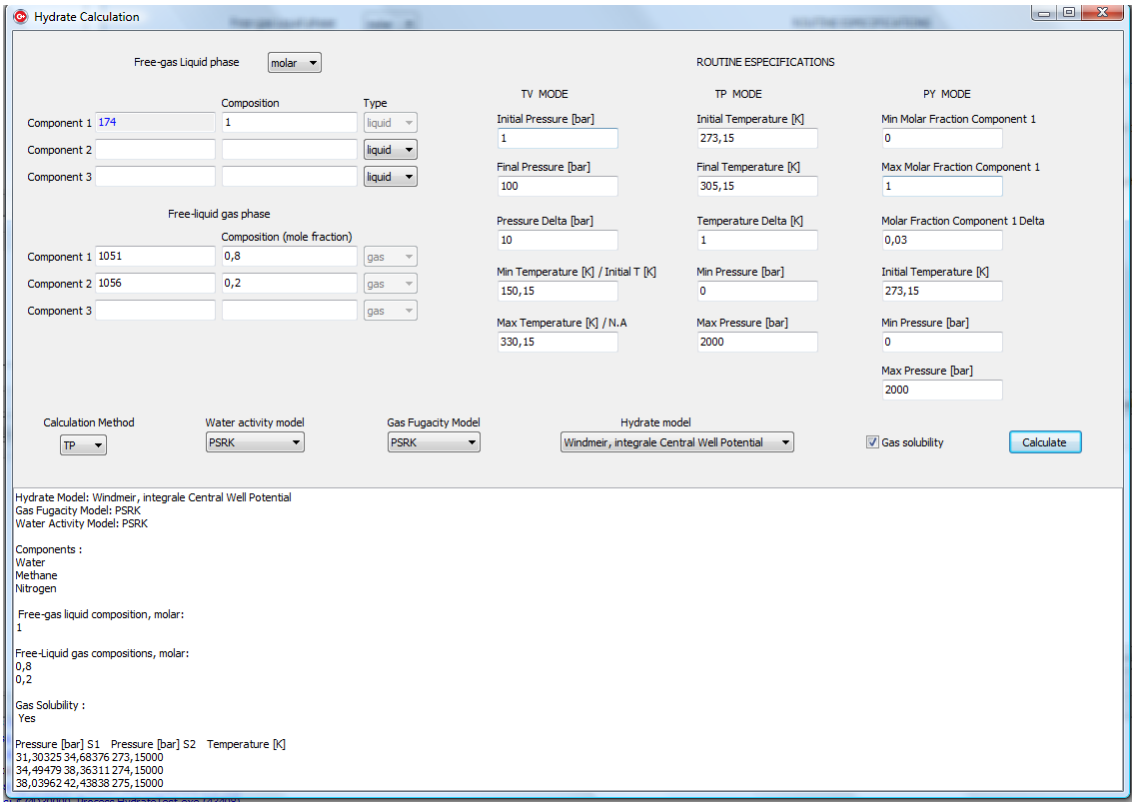

Figure 5: Developed C++ program for the hydrate prediction, including the new thermodynamic models.

Figure 5 shows the initial developed done for the thesis work, at that point 3 components in each phase could be used, being enough to predict and compare with literature data.

5. RESULTS AND DISCUSSION

Before analyzing study cases of gas hydrates in industry, the software tool has to be developed. As mentioned before, a C++ implementation of HYCAL is going to be done with some changes on it. To see if the C++ implementation is working correctly, results from both programs are going to be compared.

5.1. COMPARING HYCAL AND C++ IMPLEMENTATION

Hydrate equilibrium results by using the developed C++ implementation and the Windemeier's HYCAL program were done to observe if the new implementation shows same or similar prediction results and verify that the routine was correctly written.

Water, nitrogen (y=0.2), methane (y=0.4) and ethane (y=0.4) mixture:

Routine using PSRK model for water activity and fugacity and no solubility effects taken into consideration:

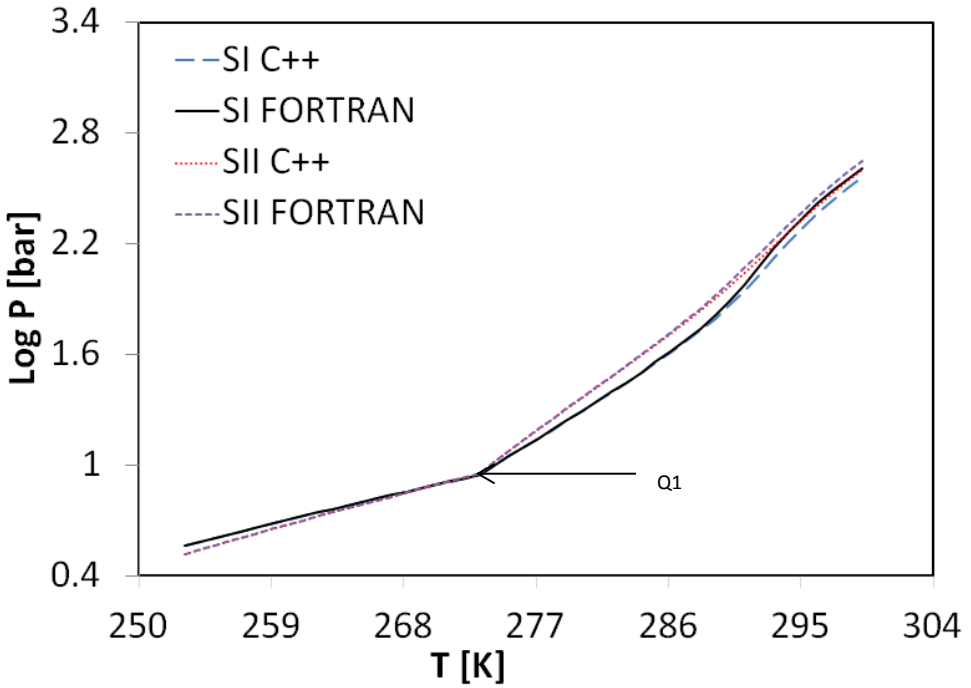

Figure 6: Comparison between Windmeier's HYCAL and the C++ implementation for a water-nitrogen-methane-ethane system, using Windmeier's integral Central Well Potential.

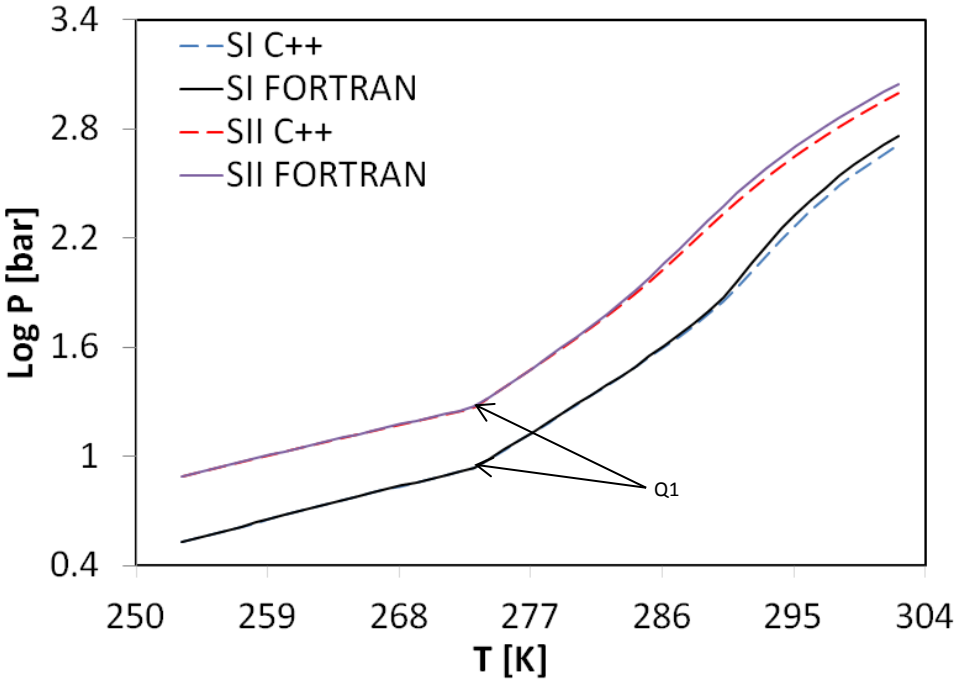

Figure 7: Comparison between Windmeier's HYCAL and the C++ implementation for a water-nitrogen-methane-ethane system, using Kihara Potential Parameter.

It can be seen that before Q1 both programs behave the same, where hydrate equilibria is predicted equally. Also both programs show the same values for Q1, which is approximately the melting point of water.

Some changes are seen after Q1 in the line L_w-H-V. Where after the melting point, at temperatures around 285K, the lines for both structures start splitting each other, with greater pressure values for HYCAL results.

Reasons attributed to the similarities are that before the melting point, the water is ice with no activity coefficient, making zero the term for the water contribution in the chemical potential calculation. Having no water contribution, removes the difference that both programs have in the methods for the water activity calculation. For the liquid-free gas phase fugacity calculations differences are not appreciable, because at conditions below the melting point, the low temperatures and moderate pressures of the gas hydrate equilibrium are such that the fugacity coefficient of the gas calculated by both programs are near one, where the gas is behaving almost as an ideal gas, making the fugacity used by both programs almost similar and thus calculations are equal.

After Q1, differences start to appear, due to the opposite reasons mentioned before. In this case water in liquid and its activity coefficient is taken into account and having water contribution adds a difference between both programs, because the difference on the thermodynamic model they use. Even though there is a difference in the activity coefficient calculation, this is not the main reason why the programs show different results. The activity coefficient is used in the calculation of the water-hydrate chemical potential difference, where depending on this value the limits of the iteration routine change, so a really big variance between both programs for the calculation of activity coefficients had to be achieved to affect the iteration, and because both programs use reviewed and accurate models, independent of which one is better, the effect won't be crucial.

This difference is thus attributed to the difference between the thermodynamic models used for the liquid-free gas fugacity coefficient calculation. At the conditions over the melting point, the hydrate equilibrium pressures start being not moderate, but high. After approximately at 280K, the equilibrium pressures are high enough to move away the ideality of the gas, affecting the values of fugacity coefficient and consequently the occupancy grade. The fugacity value is a crucial variable for the occupancy grade calculation, where differences can be propagated due to the various mathematical operations in which they take place inside the equation.

Even though there are some differences between both programs, equal predictions before Q1 and similar predictions after Q1 are achieved with the C++ implementation. Because the differences between both programs are attributed to differences in the fugacity coefficient thermodynamic model implemented, with the C++ implementation models using more powerful models, the program validation is achieved for binary mixtures, multicomponent mixtures and with mixtures using inhibitors.

5.2. COMPARING WINDMEIER'S INTEGRAL CENTRAL WELL POTENTIAL AND KIHARA POTENTIAL PARAMETERS FOR LANGMUIR'S CONSTANT CALCULATION USING C++ IMPLEMENTATION

Hydrate equilibrium results of the C++ implementation by using Integral Central Well Potential and by using Kihara Potential Parameters were obtained to compare differences between these models.

Water, nitrogen (y=0.2), methane (y=0.4) and ethane (y=0.4) mixture: Routine using PSRK model for water activity and fugacity and no solubility effects taken into consideration.

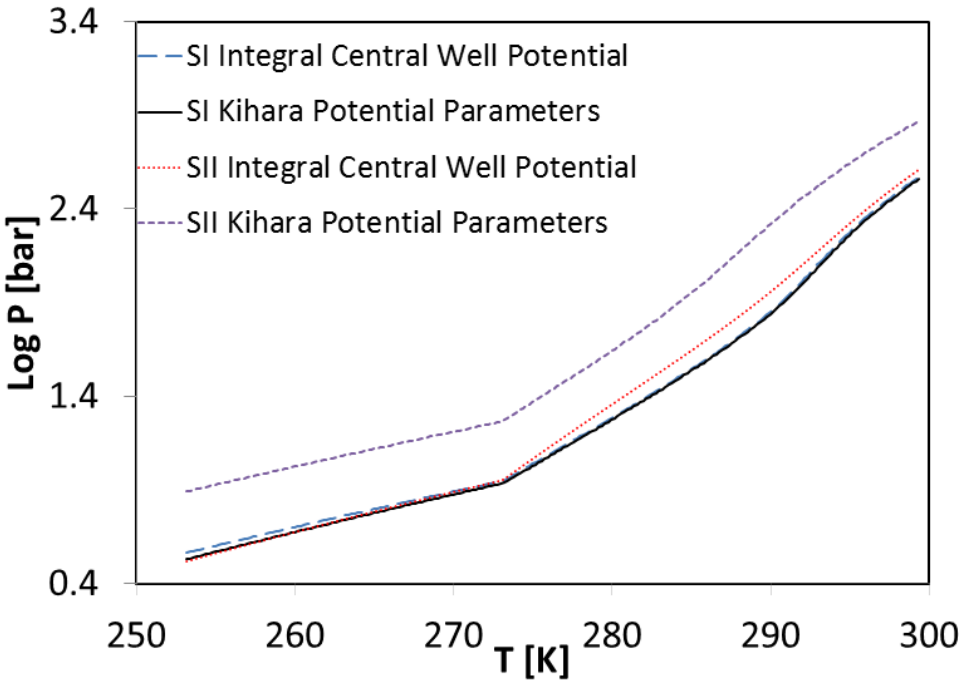

Figure 8: Comparison between hydrate models using C++ implementation for a water-nitrogen-methane-ethane system.

It can be seen that both models behave almost equally for the SI prediction, but for the SII prediction big differences are noted. At this point is not possible to select the best model, because there is no basis to know the one that fits more to reality. Because of this, a prediction for only SII is going to realized using both models and plotting the results with experimental data; the best fitted model, is going to be the chosen one.

Water-Nitrogen: Routine using PSRK model for water activity and fugacity and solubility effects taken into consideration.

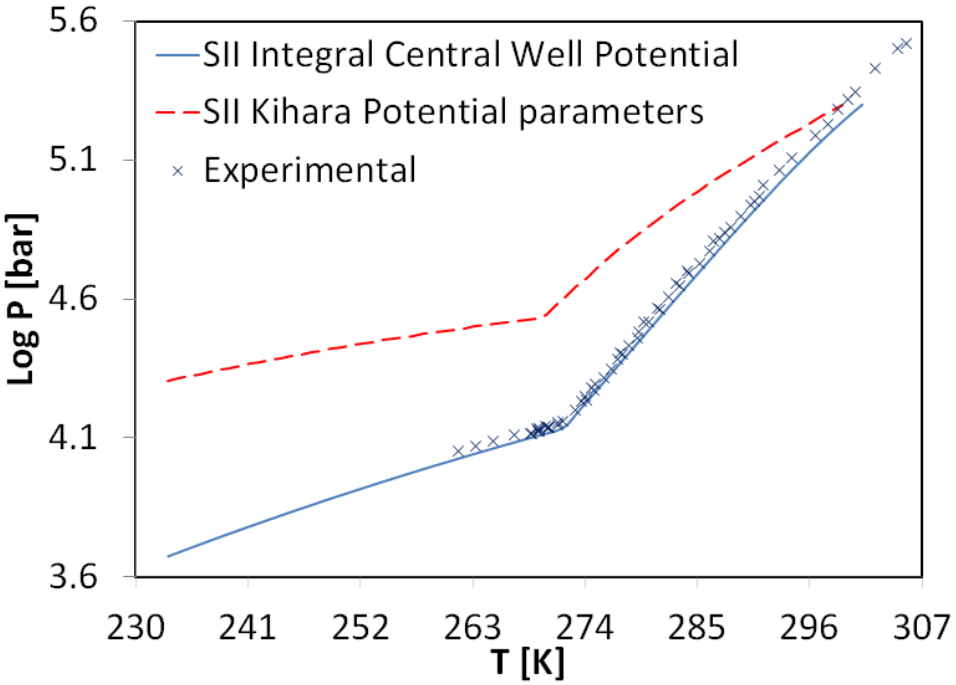

Figure 9: Comparison between hydrate models using C++ implementation for a water-nitrogen system.

It is clear that the Integral integral Central Well Potential fits better with experimental data, for this is going to be the chosen model for the prediction of hydrate equilibria and the comparison with experimental data. The better behavior of the integral Central Well Potential can be that the parameters for the prediction of SII are better fitted to the experimental known data, giving better results.

5.3. COMPARING C++ IMPLEMENTION RESULTS USING WINDMEIER'S INTEGRALLE CENTRAL WELL POTENTIAL AND EXPERIMENTAL DATA.

Hydrate equilibrium results of the C++ implementation by using Integral Central Well Potential were obtained to compare them with experimental data from DDB. Different systems were predicted, and for each system different model combinations for the calculation of fugacity and activity coefficient were studied, to examine and discuss the results.

5.3.1. NO INHIBITORS

Water and carbon dioxide:

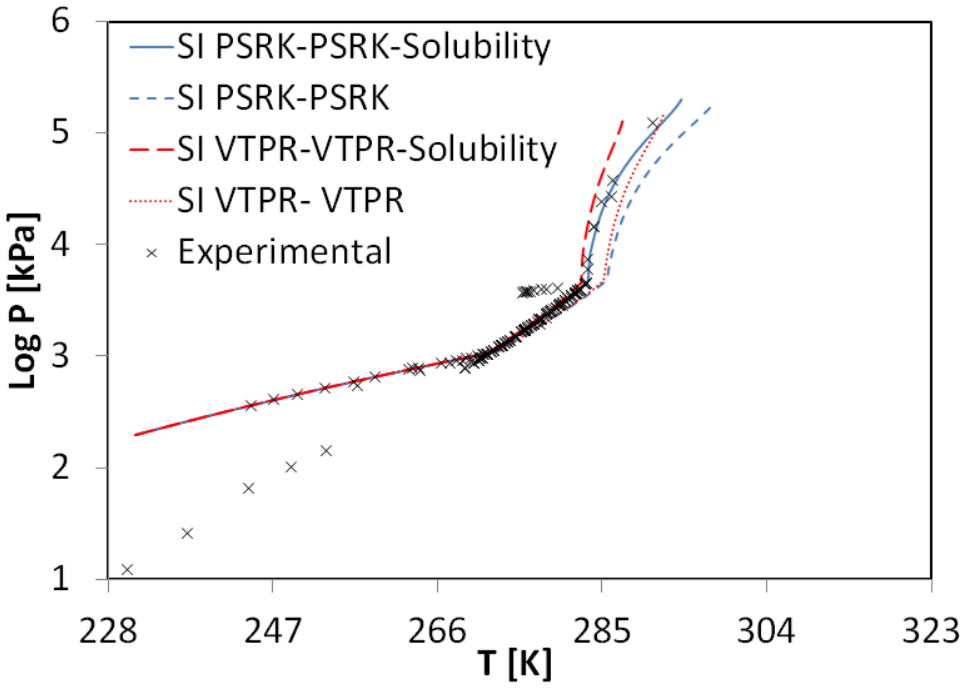

Figure 10: Comparison between C++ implementation, using the integral Central Well Potential model and experimental data from DDB for a water-carbon dioxide system.

Water and methane:

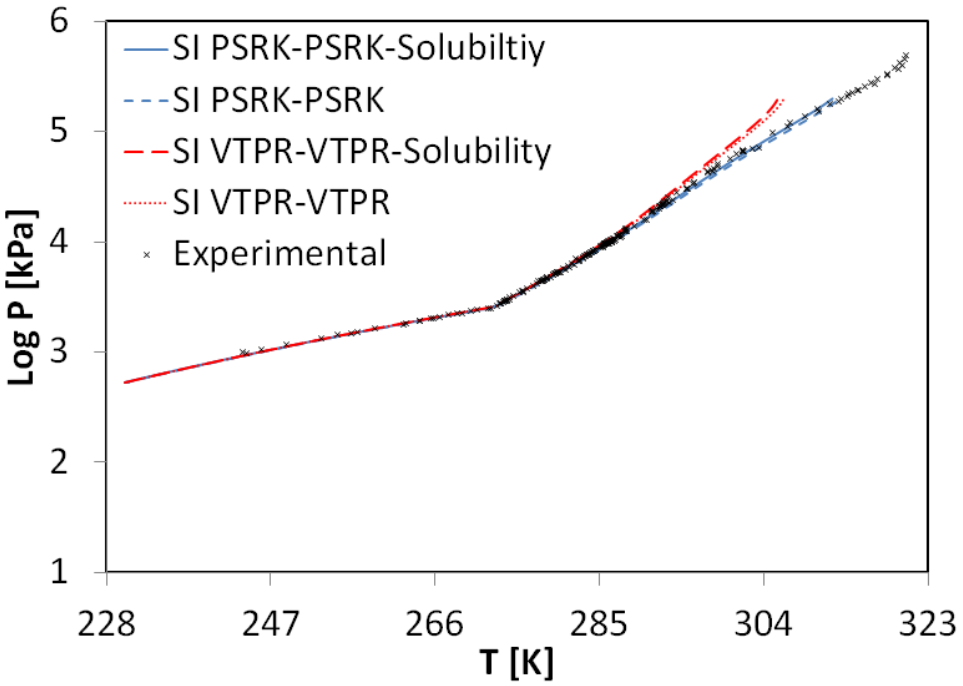

Figure 11: Comparison between C++ implementation, using the integral Central Well Potential model and experimental data from DDB for a water-methane system.

It is seen for the water-carbon dioxide system, that the models taking into account solubility predict better the hydrate equilibria. This is due to the fact that carbon dioxide is known as one of the most soluble gases in water, and to avoid this effect will be a mistake, making the prediction results not to be according with reality.

For the water-methane system is seen that the solubility of the gas has not a big effect in the hydrate prediction, but a highly better prediction is achieved using solubility. This is due to the fact that methane has low solubility in water, making the effect not as high as with carbon dioxide.

Water and ethane:

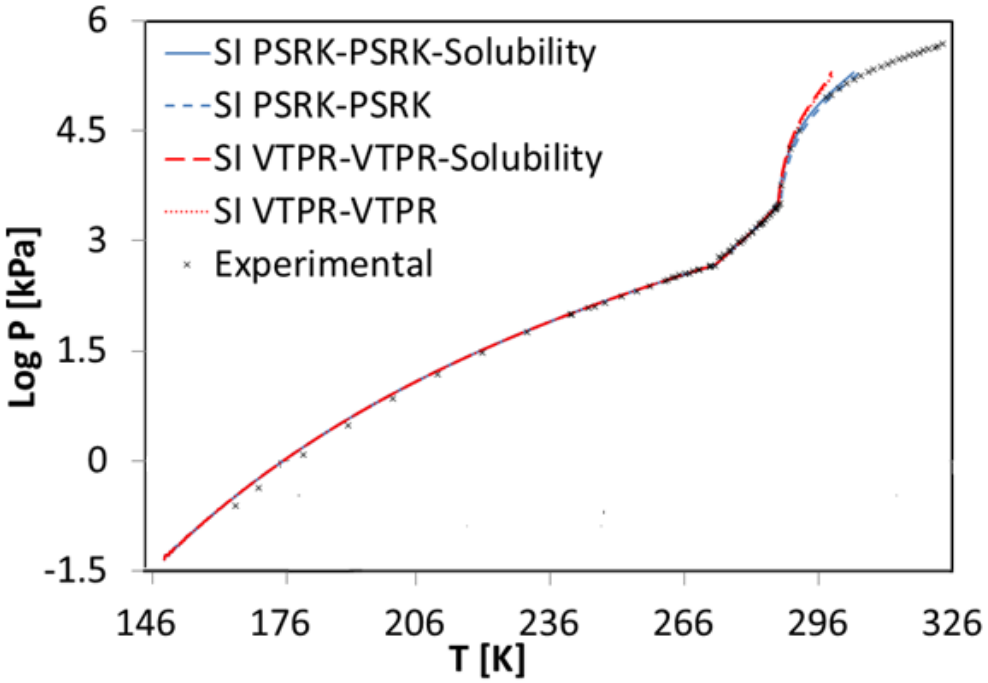

Figure 12: Comparison between C++ implementation, using the integral Central Well Potential model and experimental data from DDB for a water-ethane system.

In the water-ethane system is seen that the solubility affects the prediction only in the L_W-H- L_{HC} line. At this line, ethane is liquid and the prediction of the solubility of a liquid-liquid system at almost critical conditions is complex, and adding the fact that hydrate equilibria has to be predicted, this system is difficult to study. It is seen that at the beginning of the L_W-H- L_{HC} line, both models behave equally, but

almost at the end, close to the critical point, the model not using solubility have slightly better results.

Water and Nitrogen:

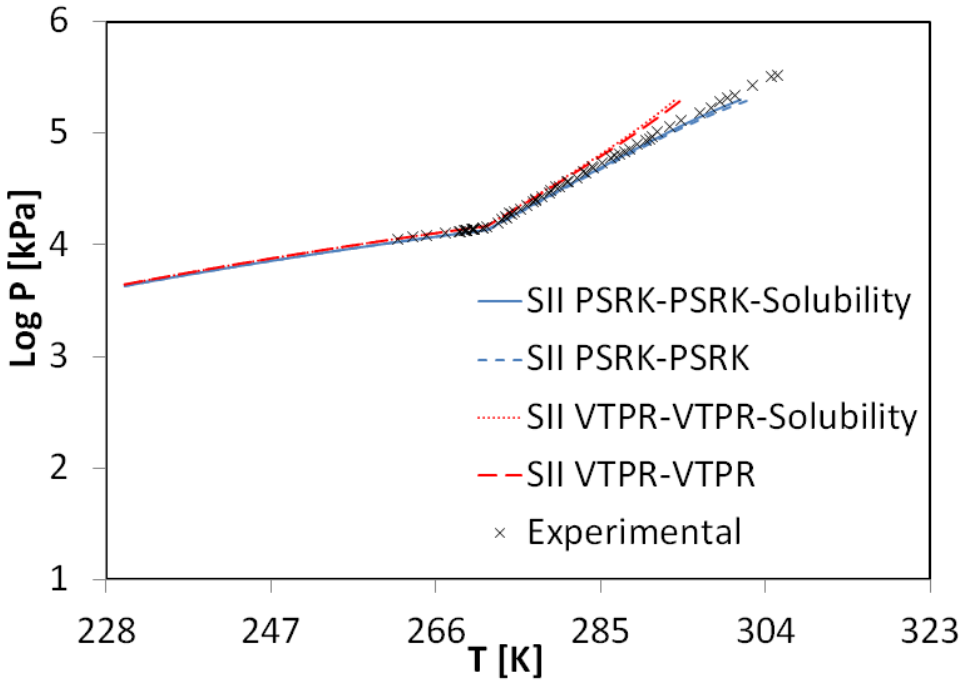

Figure 13: Comparison between C++ implementation, using the integral Central Well Potential model and experimental data from DDB for system a water-nitrogen system.

In the water-hydrogen system is seen that the solubility affects the prediction only in the L_W-H- L_{HC} line. As for the water-ethane system, differences between solubility and no solubility are small.

It can be said that solubility effects are accurately predicted, where if the solubility is not taken into account for a carbon dioxide system, prediction results will show high deviation from reality, because in reality this gas presents high solubility. On the other hand for systems with methane, ethane or nitrogen, which in reality present low solubility, it is seen that not taking this effect into account won't affect as much the prediction.

Both models gave good prediction results, but PSRK fitted better the predictions than VTPR, because of this, PSRK will be used for the prediction in the study cases, where systems water + gas without inhibition are presented.

5.3.2. INHIBITION USING ALCOHOLS

Water, methanol, methane:

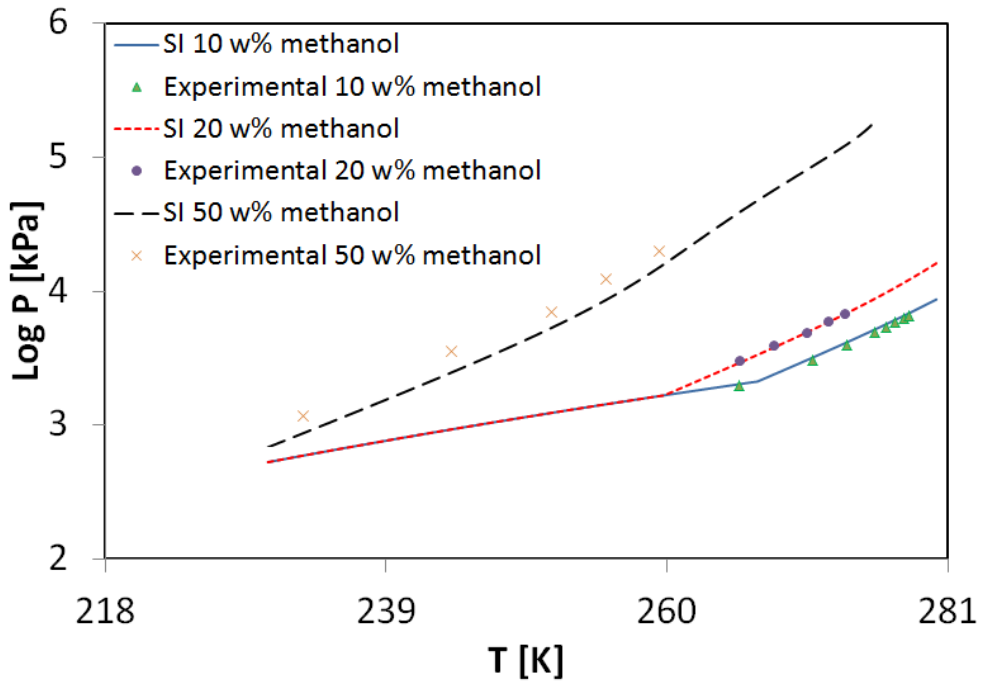

Figure 14: Comparison between C++ implementation, using the integral Central Well Potential model and VTPR and experimental data from DDB for a water-ethanol-ethane system.

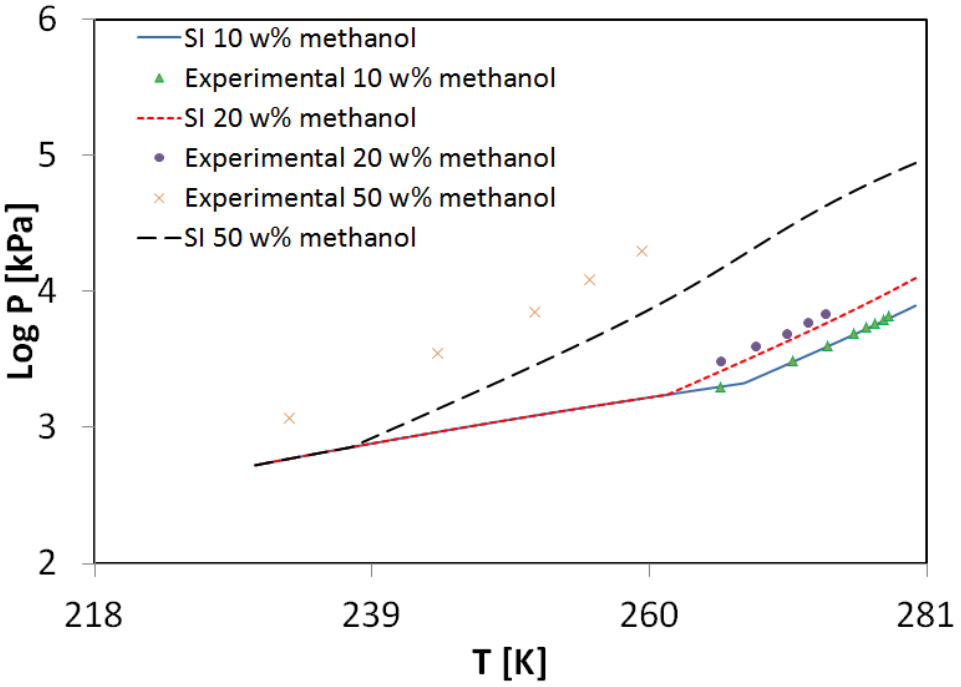

Figure 15: Comparison between C++ implementation, using the integral Central Well Potential model and PSRK and experimental data from DDB for a water-ethanol-ethane system.

VTPR and PSRK showed no big difference between the water-ethanol-ethane system prediction (seen in Appendix, figures 36 and 37), both showed highly similar results. In the case of methanol, which is one of the most common inhibitors used in industry, results using VTPR are highly better than using PSRK, where at compositions of 50%, PSRK doesn't predict accurately.

Both models gave good prediction results, but PSRK presented bad accuracy at high concentrations. In the other hand, VTPR could predict accurately the hydrate inhibition even at high concentrations of 50% mass. Because of this, VTPR will be used for the prediction in the study cases where inhibition is presented.

More systems with alcohol inhibition compared with experimental data can be found in the appendix, at the end of the work.

5.3.3. INHIBITION USING SALTS

Water, sodium chloride, methane:

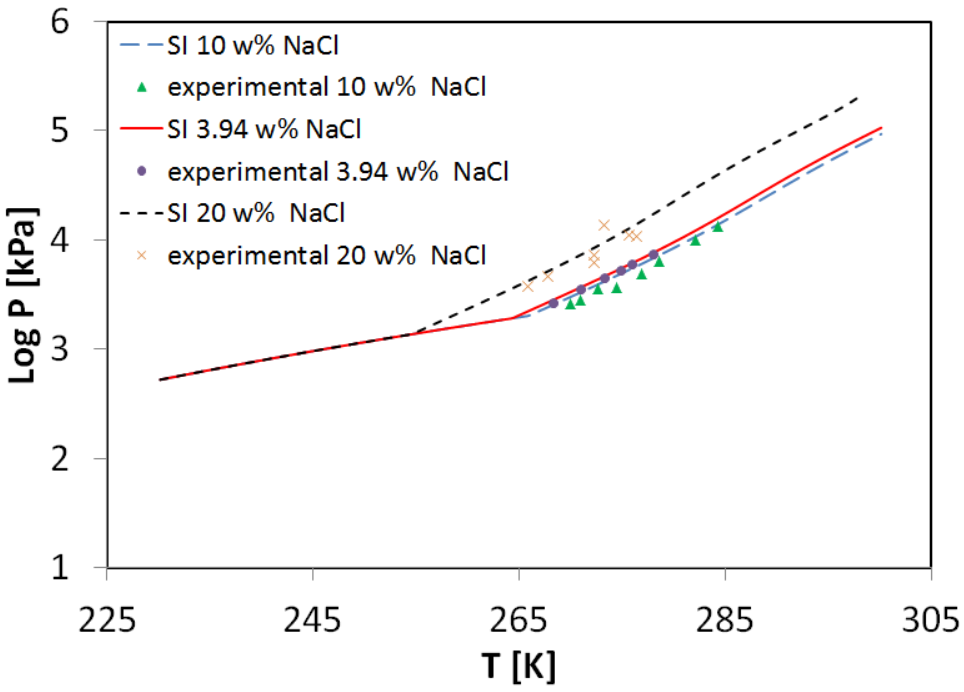

Figure 16: Comparison between C++ implementation using the integral Central Well Potential model and experimental data from DDB for a water-sodium chloride-methane system.

For the three salt systems the prediction using the PSRK-LIFAC model is highly accurate. Even for high concentrations of 20 w% of NaCl. The model presents

reliable predictions for the calculation of hydrate equilibria using salts as inhibitors, which can be used for practical purposes in industry, even at high concentrations like the ones presented in sea water.

More systems with salt inhibition compared with experimental data can be found in the appendix, at the end of the work.

6. STUDY CASES

To understand more the importance of gas hydrate equilibria prediction in industry, study cases concerning Process Engineering are going to be analyzed. In general, the study cases are focus in the natural gas production, where gas hydrates have gained all the importance and where most of the studies concerning their behavior have been accomplished. The natural gas production is going to be subdivided into three sub-processes, which are:

- Natural gas extraction.
- Natural gas treatment.
- Natural gas transport in pipe lines.

Figure 17 shows a simply description of the process with the compositions of the gas in each stage. Also, the maximum pressures and the minimum temperature presented in each stage are going to be used for the analysis, because they are the critical variables for the hydrate formation.

For the compositions in each stage, approximations to 3 components from the feed and product composition for San Juan plant [28] are going to be used, due to software limitations. These approximations do not affect the reliability of the process.

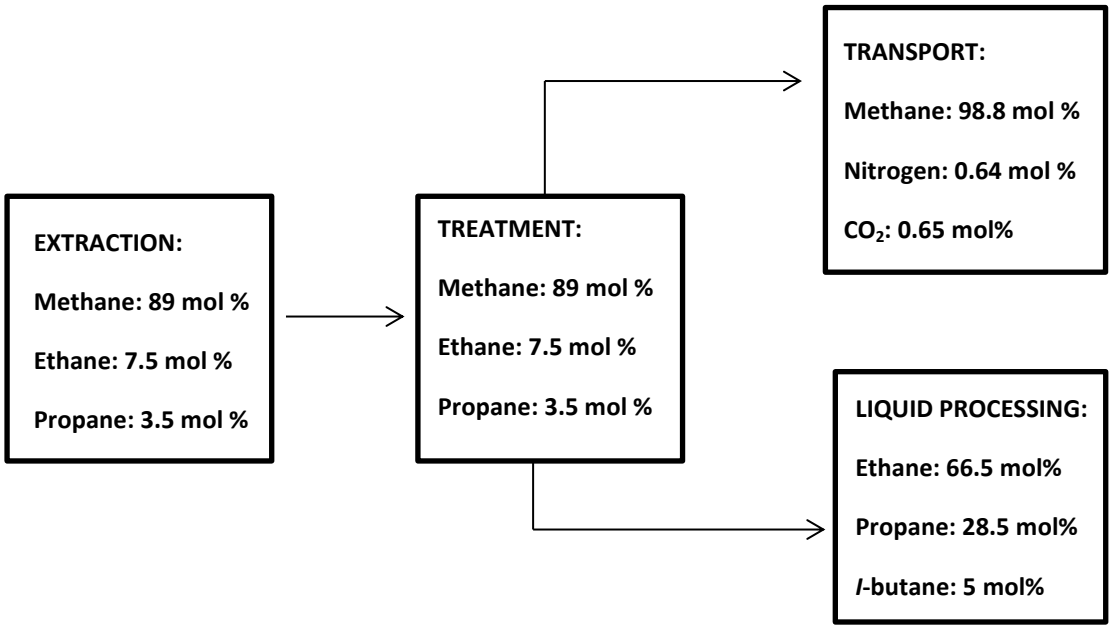

Figure 17: Natural gas production process, San Juan Plant [28].

To understand the following case study graphs, it should be remembered (as explained before), that on the left of the hydrate equilibrium line, the hydrate region exists, and to the other side hydrate is not formed. Also, for the prediction of hydrate without inhibition, PSRK will be used for the prediction of fugacity and activity coefficients and for the prediction with inhibition, VTPR will be used. The integral Central Well Potential model will be used in every case as the hydrate prediction model.

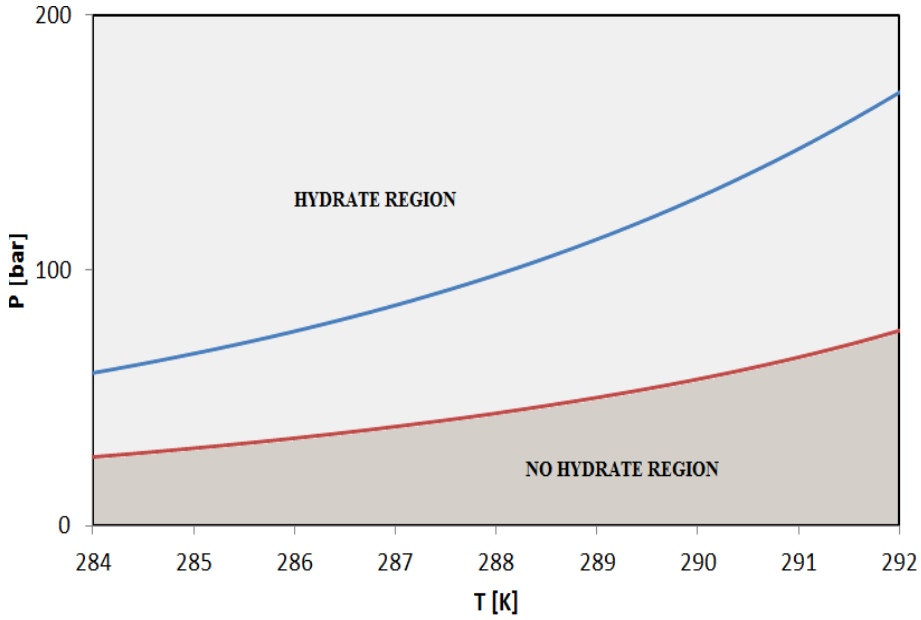

Figure 18: Gas hydrates equilibrium phases.

6.1. NATURAL GAS EXTRACTION

Hydraulic fracturing is a technique developed for natural gas extraction, consists on using high pressures via a fracturing fluid to create fractures in underground rocks, which allows liberating the retained gas. As seen in figure 19, it is needed a fracturing fluid and a proppant, where the first one is mostly 90% water plus additives and the proppant is commonly sand.

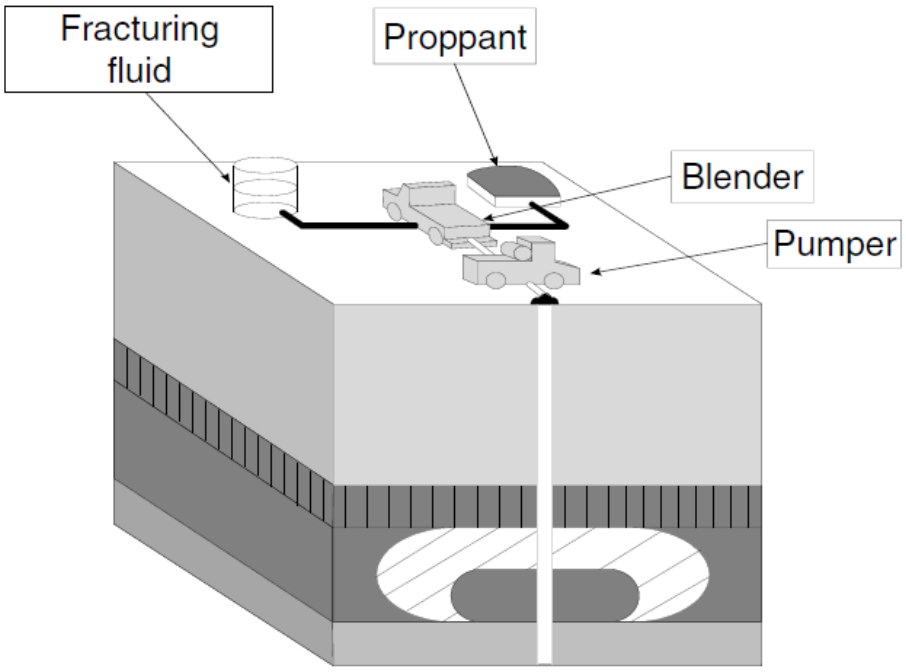

Figure 19: Hydraulic fracturing process scheme [27].

For the design of the process, the breakdown pressure of the fracture P_{bd} has to be known, this pressure is the point at which the fractures starts and depends on the properties of the rock and the depth of the well. To achieve this pressure, the fracturing fluid has to be feed at an operation pressure P_{si}, which in combination with the hydrostatic pressure of the fluid and the frictional pressure lost, gives the total breakdown pressure [27].

6.1.1. CASE STUDY

A well is located at a depth of 10000ft, where the rock is mainly sandstone. Pressure calculations have been done with a P_{bd} of 455bar and a P_{si} of 342bar [27]. The fracturing liquid composition is 90% water and 10% water-based additives. Because the additives are mainly water-based, the total composition of the liquid will be taken as water. The temperature of the water can be in the range between 283.15 K and 298.15 K, which are normal process water temperatures.

At the above conditions the hydrate formation is:

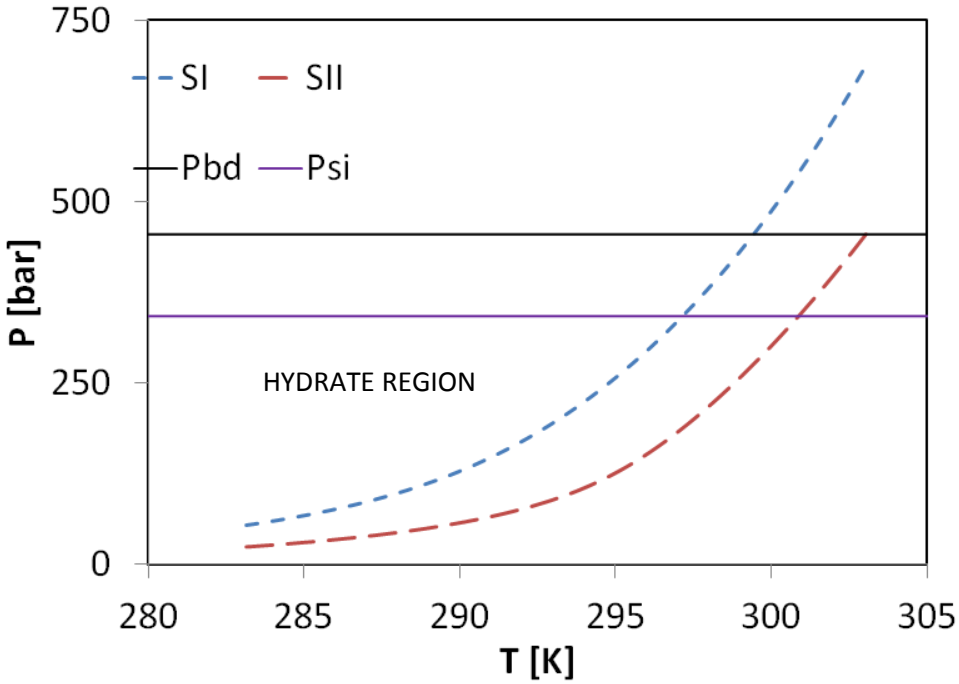

Figure 20: Hydraulic fracture with no inhibition: 89% methane, 7.5% ethane and 3.5% propane. Predicted using PSRK as thermodynamic model and integral Central Well Potential model as hydrate model.

It can be seen that the process pressures, for the temperature range, are inside the hydrate region delimited by the SII hydrate, so the risk of hydrate formation exists. This can cause plugs inside the extraction pipe line and if it is not treated, a disaster can occur, like the one on Piper Alpha in the Nord See.

To prevent hydrate formation, heating and depressurize techniques can't be used, firstly because heating a complete pipe line segment of 1000ft is impossible and second because the process pressure can't be changed, because then fracture is not achieved. So, inhibition techniques have to be used.

Glycols are going to be to study to see whether or not the hydrate prevention can be achieved, and if the conditions at which is achieved are logic. Glycols are selected due to their high boiling point, where if methanol or other alcohols are used, the further separation from the gas stream or from water represents more difficult separation processes and extra costs. Instead, with glycols easy separations can be done. Salts are just disregarded, because the hazard they can present inside the pipelines in the extraction and further natural gas treatment, due to corrosion. For this case, a 40% mass composition of EG is selected.

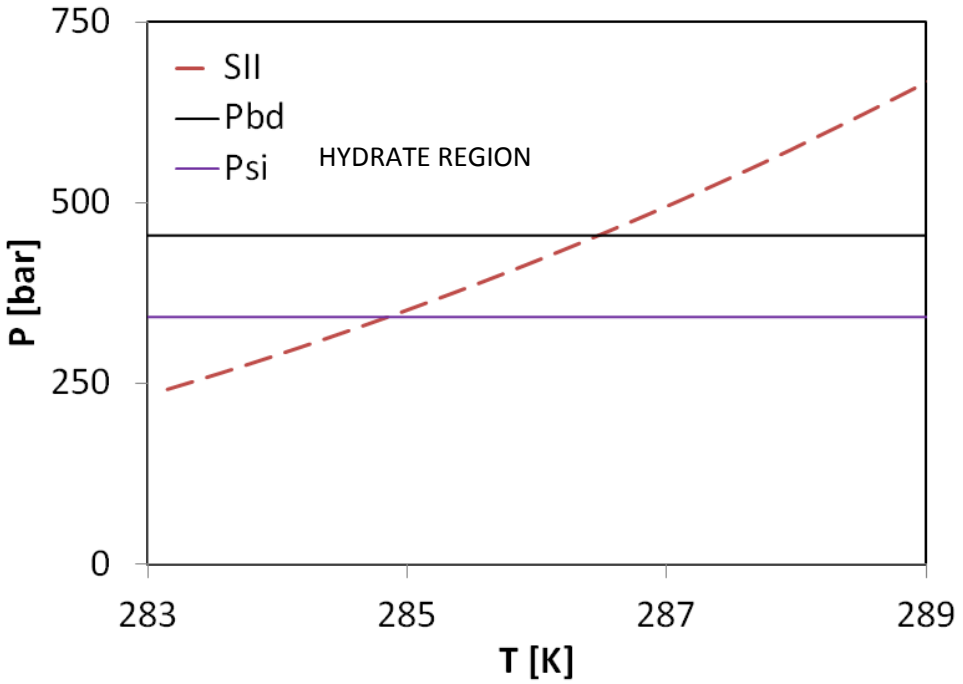

Figure 21: Gas hydrate inhibition with 40% EG. Predicted using VTPR as thermodynamic model and the integral Central Well Potential model as hydrate model.

It can be seen that with a 40% mass composition of EG, the hydrate region is moved away evading the risk of hydrate formation, by having lower pressure conditions. On the other hand, a mass composition of 40% is normal for using glycol inhibitors like EG, where certainly it represents an increase in the operations costs, but because it can be easily separated and recycled, makes it a good solution.

6.2. NATURAL GAS CONDITIONING

Figure 22 shows the typical natural gas conditioning process in industry. It can be seen that many compression stages are used, to help gas transport and to condition the gas for the separations.

Three sub-processes are going to be analyzed, which are the main processes in which water and high pressures are present, also, where literature conditions values are known. This are:

- Gas treatment.
- Dehydration.

- Liquid processing.

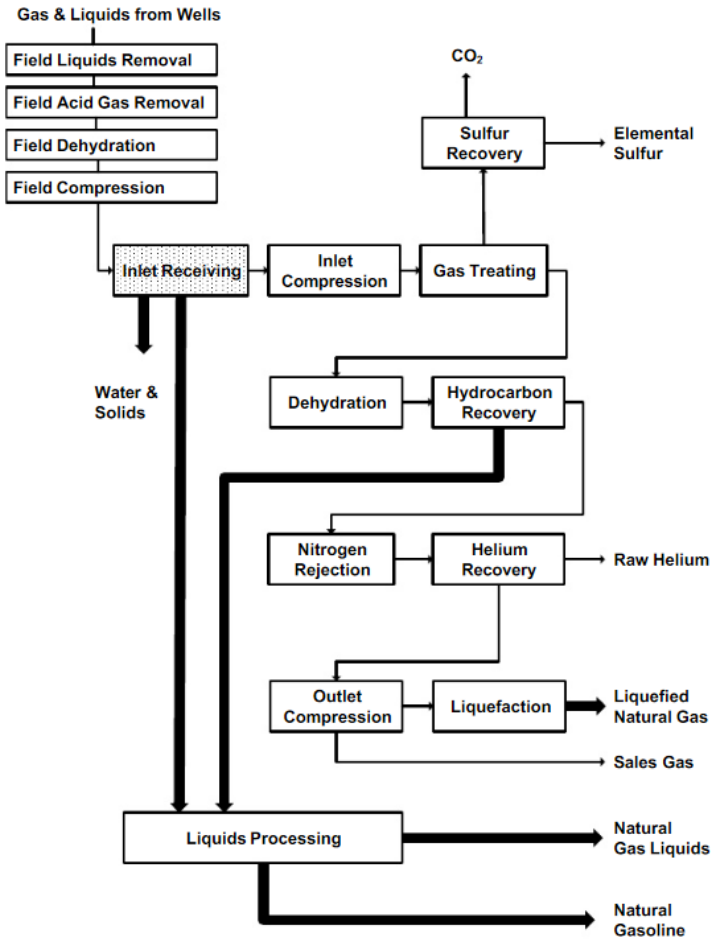

Figure 22: Typical natural gas treatment process diagram [28].

The first two processes are studied with the composition of the extraction, where the composition of methane, ethane and propane has not changed, only water and other hydrocarbons are removed. For the last one, in the hydrocarbon recovery, most of the methane is separated and the bottom composition from the de-methanizer distillation column is then processed in the liquid processing stage. Because of this, this stage is going to be analyzed using the down composition obtained in the gas treatment (see figure 17).

6.2.1 GAS TREATMENT CASE STUDY

A stream of gas is going to be treated to remove acid gases, such as hydrogen sulfide and carbon dioxide. After the inlet compression, the stream has a pressure of 60 bar and during the process the minimum temperature is in the inlet, where the gas is feed at 295.15 K [28].

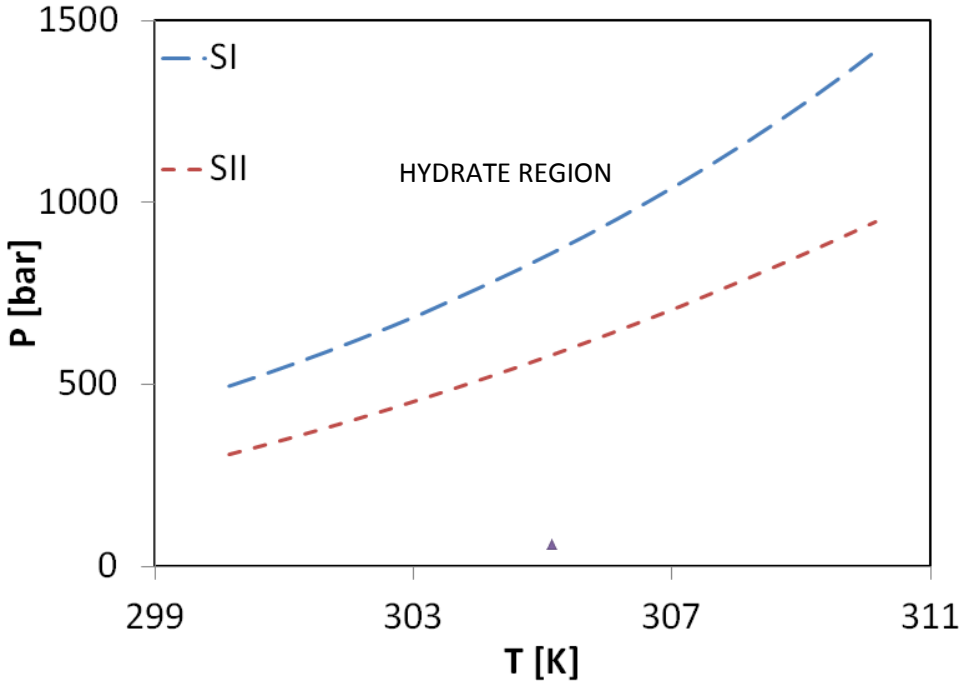

Figure 23: Gas treatment: 89% methane, 7.5% ethane and 3.5% propane. Predicted using PSRK as thermodynamic model and the integral Central Well Potential model as hydrate model.

It is noticed, that the process conditions are safe and hydrate will never be formed in the gas treatment stage. Also, hydrate formation due to high pressures in the process are avoided, because the hydrate formation pressures are relatively high.

6.2.2 DEHYDRATION CASE STUDY

In the dehydration, absorption at 60 bar takes place, where low temperatures help the absorption, but elevates the risk of hydrate formation. For this case study, temperature limits are going to be analyzed.

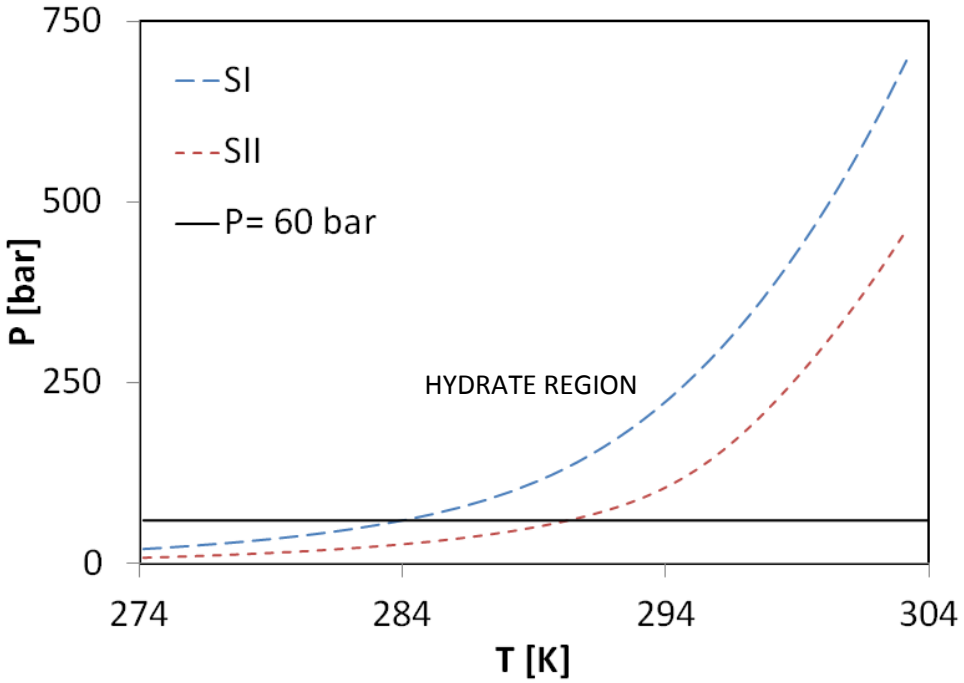

Figure 24: Dehydration: 89% methane, 7.5% ethane and 3.5% propane. Predicted using PSRK as thermodynamic model and the integral Central Well Potential model as hydrate model.

It can be seen that a 60 bar SII hydrate is formed around 290.15 K, with SI structure. Because of this, the absorption process has to be done at temperatures of 291.15 K or more.

Industrially, absorption process for dehydration consists of using a glycol (TEG commonly) and temperatures near ambient (298.15 K), so the use of inhibitors is not required, and the only control that has to be done is to assure that the temperature doesn't reach 290.15 K or below.

6.2.3. HYDROCARBON RECOVERY-LIQUID PROCESSING CASE STUDY

In this stage, methane is separated from the other hydrocarbons in the de-methanizer column. The bottom stream, richer in heavier hydrocarbons, goes through further separations depending of the objectives of the company, which can be ethane production, propane production or $+C_4$ hydrocarbon fuels. For this, cooling processes using compression and expansions or cryogenic distillations are used to separate the different hydrocarbons depending on their boiling point. From Daniel measurements and control application notes [29], the feed with a pressure

of 27.6 bar and a temperature of 294.25 K presents the most critical conditions in the process, conditions to which the hydrate formation prediction will be study.

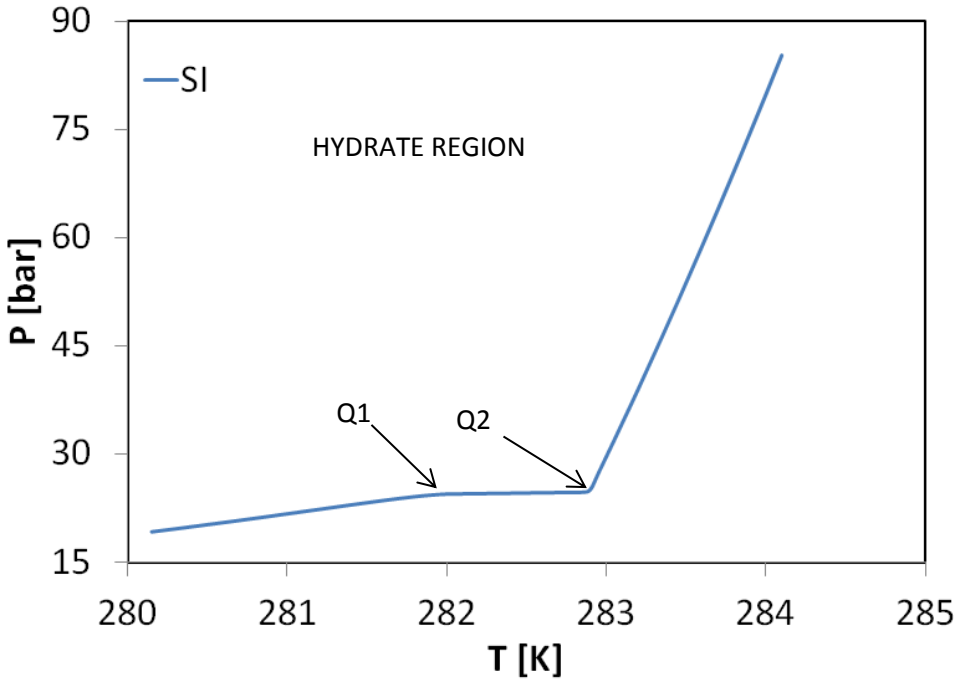

Figure 25: Liquid Processing: 66.5% ethane, 28.5% propane and 5% *i*-butane. Predicted using PSRK as thermodynamic model and the integral Central Well Potential model as hydrate model.

It is seen that at the conditions of the gas treatment, the hydrate formation is not possible, thus no inhibition methods are needed. A hydrate risk can exist just if the temperature is around 283.15 K.

6.3. NATURAL GAS PIPE LINE

After the natural gas treatment most of the total water content is removed to prevent hydrate formation inside the supply pipe lines. The following case study deals with possible water content in the natural gas and gives an extra precaution for the conditions inside the pipe lines.

6.3. CASE STUDY

From the Gas Pipe Lines Operation Manual [30], normal operation pressure for pipe lines are between 110 and 160 bar, and for this case a pressure of 150 bar is

going to be studied. Additionally, a pressure ratio of 1.35 between intermediate compressor stations is going to be used, giving an outlet pressure of 111.11 bar.

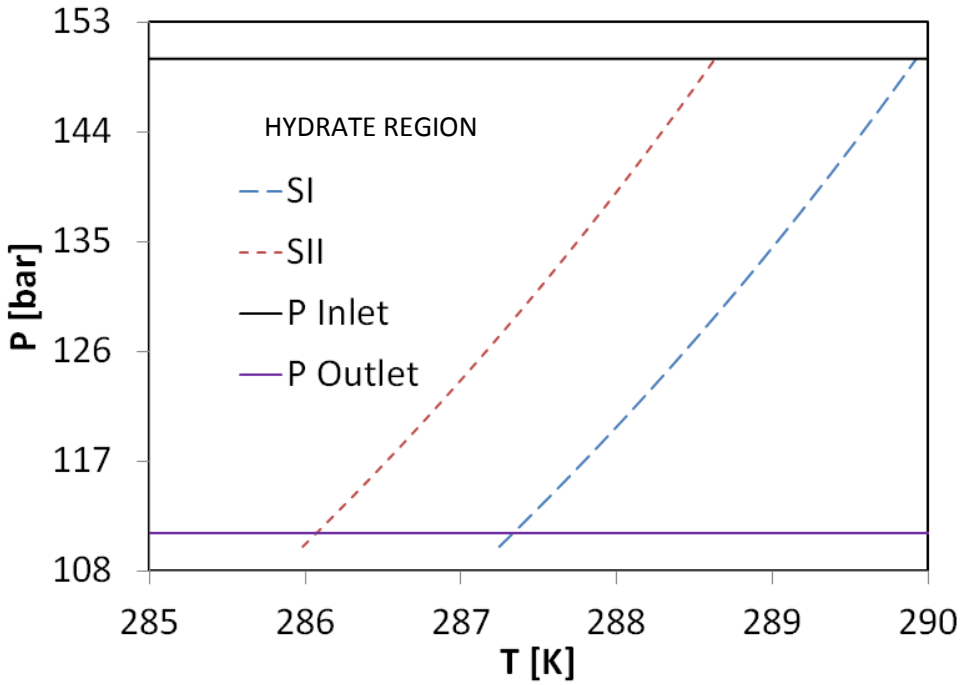

Figure 26: Pipe line with no inhibition: 98.8% methane, 0.64% nitrogen and 0.56% carbon dioxide. Predicted using PSRK as thermodynamic model and the integral Central Well Potential model as hydrate model.

It can be seen that the hydrate region is delimited by the SI hydrate, where to the right of the equilibrium line the risk of having hydrate formation exists. So for this process keeping the initial temperature over 288.15 K and the outlet temperature over 287.15 K is crucial.

In some conditions, for example in Yamburg, Siberia, the third biggest natural gas field of the world, temperatures of 243.15 K are normal in winter times, additionally it is a permafrost region, making the pipe lines to be exposed to below zero conditions, even underground. These conditions can cool down the natural gas and even enter the hydrate region. For this case an average temperature of 283.15 K inside the pipe line is going to be selected for its study, where looking at figure 26, it is more than noticed that 283.15 K is inside the hydrate region.

Because the risk of having hydrate formation exists, inhibition using methanol is going to be used, because heating kilometers of pipe lines is unreasonable and

the pressure is needed for transporting, so heat and pressure inhibition options are rejected. Also, other alcohols or glycols represent problems for the compressions stages, because they are presented in liquid phase. On the other hand, salts represent a danger due to corrosion and solid accumulation inside pipe lines. Hydrate formation with a methanol mass composition of 20% is predicted as follow. The composition of the gas phase will have a change for the prediction, because the interaction parameter between nitrogen and methanol for the VTPR model is unknown, so the nitrogen composition will be added to the carbon dioxide.

The inhibition is predicted as follow:

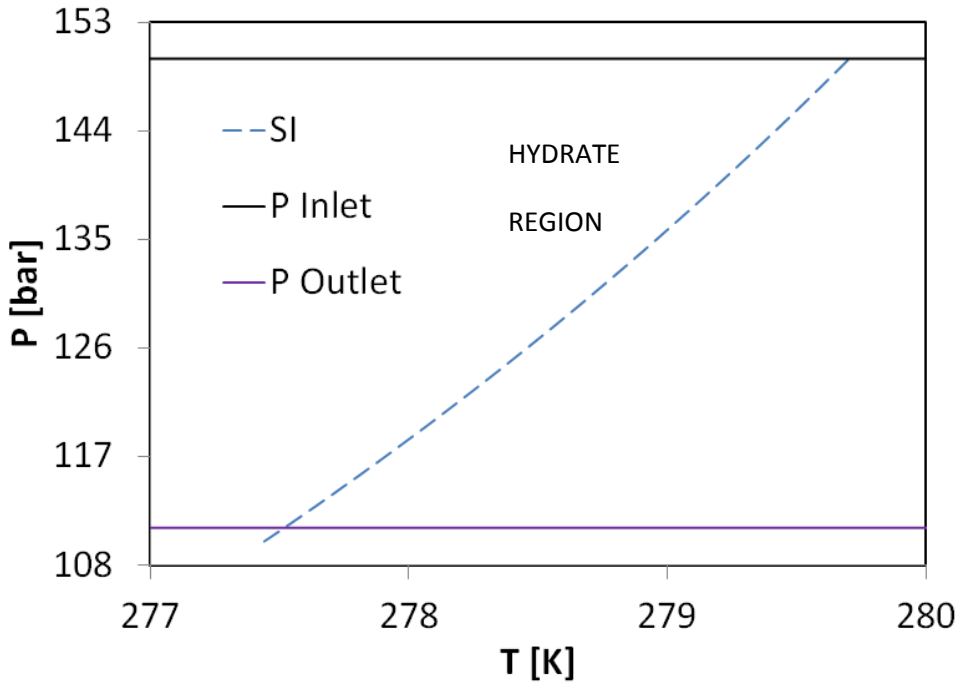

Figure 27: Gas hydrate inhibition with 20% mass methanol. Predicted using VTPR as thermodynamic model and the integral Central Well Potential model as hydrate model.

It can be seen that using methanol moves the hydrate equilibria to the left, away from the process conditions, where now the hydrate formation is avoided. Also, the concentration of methanol is not so high and it is accorded to normal inhibition compositions. Although the hydrate is prevented, it is better to use more amounts of methanol, to have an extra prevention.

7. SUMMARY

Based on the on the work of Rock and Windmeier's former tool HYCAL and with the help of the DDB thermodynamic models routines PSRK, VTPR and PSRKLIFAC, an improved C++ implementation was made for the gas hydrates prediction.

As it can be seen in chapter 5, figures 10 to 16, and in Appendix, figures 34 to 39, prediction results were compared with literature data, presenting high accuracy in the calculations. The studied systems cover all the possible systems to study, which are: non-inhibited systems with single gas or mix of gases in the free-liquid gas phase, inhibited systems using alcohols or glycols with single gas or mix of gases in the free-liquid gas phase and inhibited systems using salts with single gas or mix of gases in the free-liquid gas phase.

The importance of gas hydrates in natural gas production was taken as case study for the present work. Figure 20 shows that the extraction of this resource occurs inside the gas hydrate formation region, so inhibition methods have to be used. In figure 21, a solution for this process is presented, using 40% mass composition of EG as inhibitor and moving away the hydrate region from the process conditions. Figures 23, 24 and 25, show that the natural gas conditioning process is safe from hydrate formation, only certain precautions have to be taken into account, like not allowing temperatures of 290.15 K or below in the dehydration stage. Figure 26 shows that in the case of having water inside a pipe line during natural gas transportation, the system will be inside the gas hydrate formation region. Figure 27 presents a solution using 20% mass composition of methanol as inhibitor, where the gas hydrate region is moved away from temperatures around 283.15 K. Using more amounts of methanol, will move hydrate risk even farther away from the pipe lines conditions.

All those study cases represent exactly the importance of gas hydrates in industry. The first one presents an inhibition solution for a process which the conditions of temperature and pressure can't be changed. The second allows engineers designing a process, to know that the process conditions are safe from gas hydrate formation. Also, allows them to know the risk conditions to avoid. In the

last one, a possible hydrate formation case is presented, where a solution using inhibition is given, allowing a company to have a prevention instead of a future problem. Understanding the behavior of gas hydrates gives industry and engineers the advantage of overcoming future problems.

Natural gas is just one example for gas hydrate application, different processes can present this risk. More examples of gas hydrate can be studied, not only as a problem limitation for some processes, but also as a benefit. More examples for studying gas hydrates are:

- Gas hydrates as a gas transport medium.
- Gas hydrates as a solution for carbon dioxide storage.
- Extraction of methane from natural gas hydrate's wells.
- Gas hydrates formation in expansion valves.

Also, more gases forming gas hydrates can be studied and fitting parameters for their applicability in the current models can be done, in this way, the gas hydrate prediction can be enriched.

8. LITERATURE

1. SLOAN, D., KOH, A.: Hydrates of Natural Gases, third Edition, CRC Press, Taylor & Francis Group, Boca Raton, Fl, 2008

2. WINDMEIER, C.: Doctoral Thesis, Experimentelle und theoretische Untersuchungen zum Phasen- und Zersetzungverhalten von Gashydraten, Universität Fridericiana zu Karlsruhe, Karlsruhe, 2009.

3. ROCK, A.: Doctoral Thesis, Experimentelle und theoretische Untersuchung zur Hydratbildung aus Gasgemischen in inhibitorhaltigen wässrigen Lösungen, Universität Fridericiana zu Karlsruhe, Karlsruhe, 2002.

4. DAVY, H.: The Bakerian lecture: On some of the combinations of oxymuriatic gas and oxygen, and on the chemical relations of these principles, to inflammable bodies. *Phil. Trans. Roy. Soc. London* 101 (1811), 1-35.

5. HAMMERSCHMIDT, E. G.: Formation of gas hydrates in natural gas transmission lines. *Ind. Eng. Chem*. 26 (1934), 8, 851-855.

6. KATZ, D. L.: Prediction of conditions for hydrate formation in natural gases. Am-*Inst. Mining Met. Engrs.,* 160 (1945).

7. STACKELBERG VON, M.: Feste Gashydrate. *Naturwissenchaften* 36 (1949).

8. STACKELBERG VON, M ; MÜLLER, H. R.: Feste Gashydrate. II. Struktur und Raumchemie. *Zeitschrift für Elektrochemie* 58 (1954), 1, 25 – 39.

9. VAN DER WAALS, J. H. ; PLATTEEUW, J.C.: Clathrate Solutions. Prigogine, I. (Hrsg.): *Advances in Chemical Physics* Bd. II., Interscience Publishers Inc., New York, 1959, 1-57.

10. BONIFACE, A.: Hydrates – a factor for Piper Alpha? *TCE – The Chemical Eng.,* (1990), 12-14.

11. AMODU. A. A.: Master Thesis, Drilling through gas hydrate formations: possible problems and suggested solutions, Texas A&M University, Texas, 2008.

12. KLAUDA, J. B.: SANDLER, S. I: Global distribution of methane hydrate in ocean sediment. In: *Energy & Fuels* 19 (2005), 2, 459-470.

13. SCHMID, B., GMEHLING, J.: From van der Waals to VTPR: The systematic improvement of the van der Waals equation of state, *J. Supercritical Fluids*, 55 (2010), 438-447.

14. GMEHLING, J.: From UNIFAC to modified UNIFAC to PSRK with the help of DDB, *Fluid Phase Equilib*., 107 (1995), 1-29.

15. WEIDLICH, U., GMEHLING, J.: A Modified UNIFAC Model. 1. Prediction of VLE, h E and γ^{∞}. *Ind. Eng. Chem. Res.,* 26 (1987), 1372-1381.

16. KIEPE, J., HORSTMANN, S., FISCHER, K., GMEHLING, J.: Application of the PSRK Model for Systems Containing Strong Electrolytes, *Ind. Eng. Chem. Res.,* 43 (2004), 6607-6615.

17. HURON, M.-J., VIDAL, J.: New mixing rules in simple equations of state for representing vapour–liquid equilibria of strongly non-ideal mixtures, *Fluid Phase Equilib.,* 3 (1979) 255–271.

18. MICHELSEN, M.L.:, A modified Huron–Vidal mixing rule for cubic equations of state, *Fluid Phase Equilib.,* 60 (1990), 213.

19. HOLDERBAUM, T., GMEHLING, J.: PSRK: a group contribution equation of state based on UNIFAC, *Fluid Phase Equilib.,* 70 (1991), 251–265.

20. MATHIAS, P.M., COPEMAN, T.W.: Extension of the Peng–Robinson equation of state to complex mixtures: evaluation of the various forms of the local composition concept, *Fluid Phase Equilib.,* 13 (1983), 91–108.

21. HORSTMANN, S., JABLONIEC, A., KRAFCZYK, J., FISCHER, K., GMEHLING, J.: PSRK group contribution equation of state: comprehensive revision and extension IV, including critical constants and α- function parameters for 1000 components, *Fluid Phase Equilib.,* 227 (2005), 157-164.

22. FISCHER, K., GMEHLING, J.: Further development, status and results of the PSRK method for the prediction of vapor-liquid equilibria and gas solubilities, *Fluid Phase Equilib*., 112 (1995), 1-22.M

23. PENELOUX, A., RAUZY, E., FREZE, R.: A consistent correction for Redlich–Kwong–Soave volumes, *Fluid Phase Equilib*., 8 (1982), 7–23.

24. CHEN, J., FISCHER, K., GMEHLING, J.: Modification of PSRK mixing rules and results for vapor–liquid equilibria, enthalpy of mixing and activity coefficients at infinite dilution, *Fluid Phase Equilib*., 200 (2002), 411–429.

25. SCHMID, B., GMEHLING, J.: Revised parameters and typical results of the VTPR group contribution equation of state, *Fluid Phase Equilib*., 317 (2012), 110-126.

26. Dortmund Data Bank 2014, DDBST GmbH. http://www.ddbst.com.

27. GUO, B., LYONS, W., GHALAMBOR, A.: 17 - Hydraulic Fracturing, In Petroleum Production Engineering, *Gulf Professional Publishing*, Burlington (2007), 251-265.

28. KIDNAY, A., PARRISH, W.: 200 – Fundamental of Natural Gas Processing, *Mechanical Engineering A series of Textbooks and Reference Books*, Ohio (2006).

29. DANIEL MEASUREMENT And CONTROL, INC.: Dan Technologies Natural Gas Processing NGL Fractionation Vapor Phase Samples**,** Daniel Measurement and Control Notes, 2010**.**

30. TOTAL OIL MARINE ST. FERGUSON TERMINAL: Gas Pipelines Operation Manual, 1996

31. VAN DER WAALS, J.D.: Doctoral Thesis, Leiden, 1873.

32. SOAVE, G.: Equilibrium constants from a modified Redlich–Kwong equation of state, *Chem. Eng. Science 27*, (1972), 1197.

33. PENG, D.Y., ROBINSON, D.B.: A new two-constant equation of state, *Ind. Eng. Chem. Fund.*, 15 (1976), 59.

34. AHLERS, J., GMEHLING, J.: Development of a universal group contribution equation of state: I. Prediction of liquid densities for pure compounds with a volume translated Peng–Robinson equation of state, *Fluid Phase Equilib*., 191 (2001), 177–188.

35. LAZZUS, J.A.: Optimization of a cubic equation of state and van derWaals mixing rules for modeling the phase behavior of complex mixtures, *Revista Mex. de Fisica*, 58, (2012), 510-514.

9. APPENDIX

9.1. NOMENCLATURE

d	Total differential sign
i	Type of cage
J	Type of element
E	Grand canonical partition function for water
A	Helmholtz free energy of empty host lattice
β	Property of the empty hydrate crystal
k	Boltzmann's constant
T	Temperature
$q_{J,i}$	Partition function of a *J* molecule in a type *i* cavity
λ_J	Chemical activity of the guest *J*
S	Entropy
P	Pressure
V	Volume
$v_i * N_W$	Total number of cavities
μ_W^H	Chemical potential of water in hydrate form
$\theta_{J,i}$	Probability of finding a molecule of type *J* in a cavity of type *i*,
f_J	Fugacity of component *J*
μ_W^β	Chemical potential of the host
$C_{J,i}$	Langmuir constant
$\Delta\mu_W^{\beta-L}$	Difference of the chemical potential of water between empty hydrate and liquid form
$\Delta\mu_W^{H-L}$	Difference of the chemical potential of water between hydrate and liquid form
a_w	Water activity

$\Delta\mu_W^{H-\alpha}$	Difference of the chemical potential of water between hydrate and ice form
R	Free cavity radius
$\Phi(r)$	The pair potential energy
a	Radius of the guest molecule from the cavity center
r	Distance of the guest molecule from the cavity center
ε	Maximum attractive potential at, $r = \sqrt[6]{2 * \sigma}$
σ	Cores distance at zero potential
δ^N	Parameter for the cell potential calculation
z	The coordination number (number of water molecules) of the cavity
a	Parameter which takes into account the attractive forces
v	Specific volume
b	Closest packing volume
T_r	Reduced temperature
γ	Activity coefficient
Γ	Group activity coefficients

9.2. MORE RESULTS

9.2.1. COMPARING PROGRAMS

Water and methane mixture: TP routine using PSRK model for water activity and fugacity and no solubility effects taken into consideration:

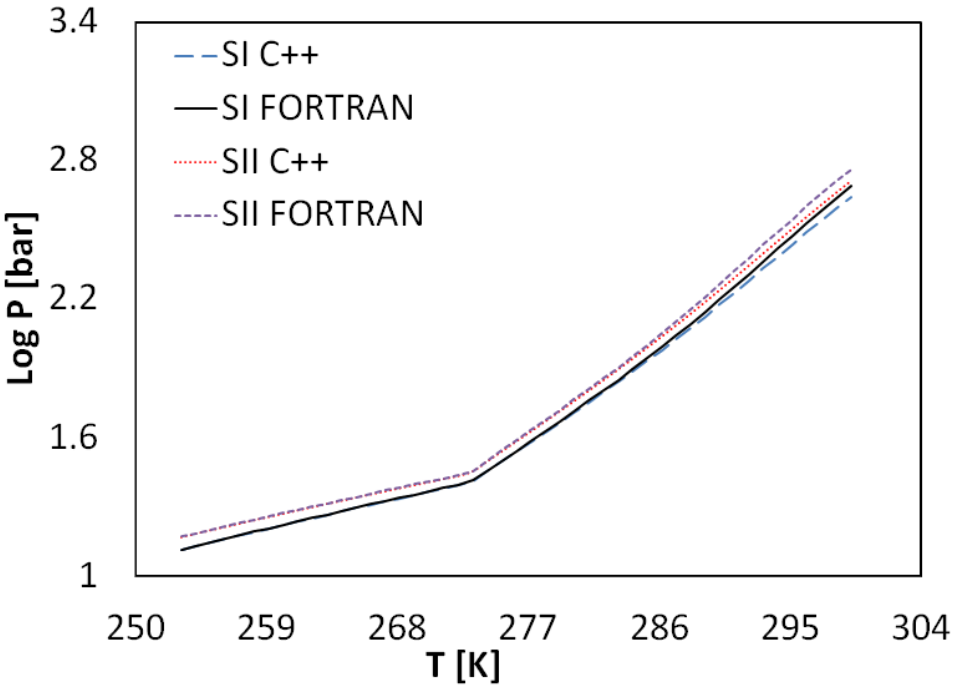

Figure 28: Comparison between Windmeier's HYCAL and the C++ implementation for a water-methane system, using the integral Central Well potential.

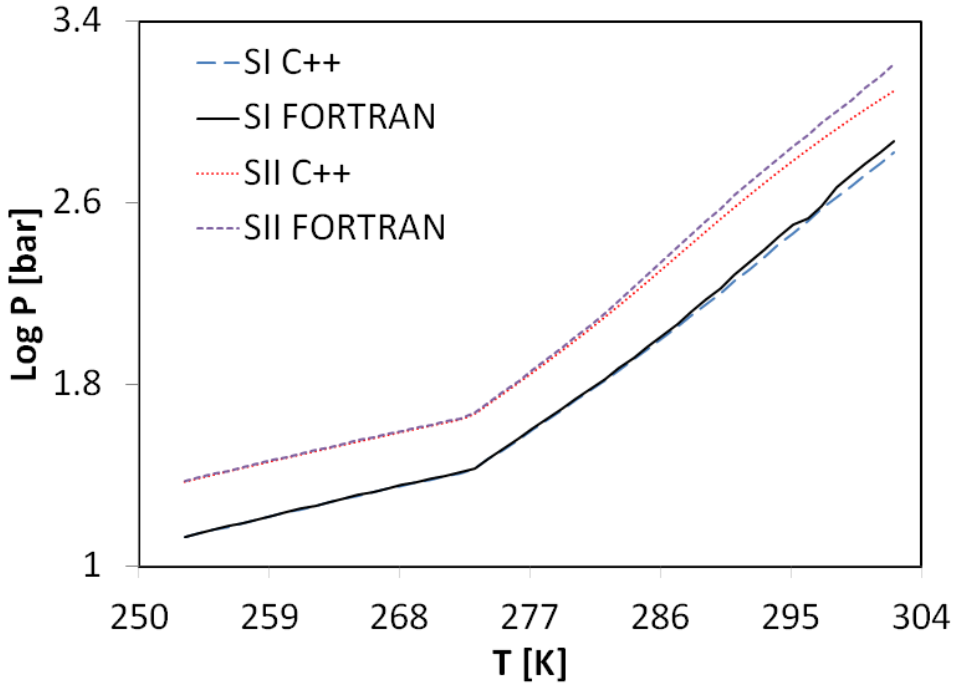

Figure 29: Comparison between Windmeier's HYCAL and C++ implementation for a water-methane system, using Kihara Potential Parameters.

Water (x=0.9), ethanol (x=0.1) and methane mixture: TP routine using PSRK model for water activity and fugacity and no solubility effects taken into consideration:

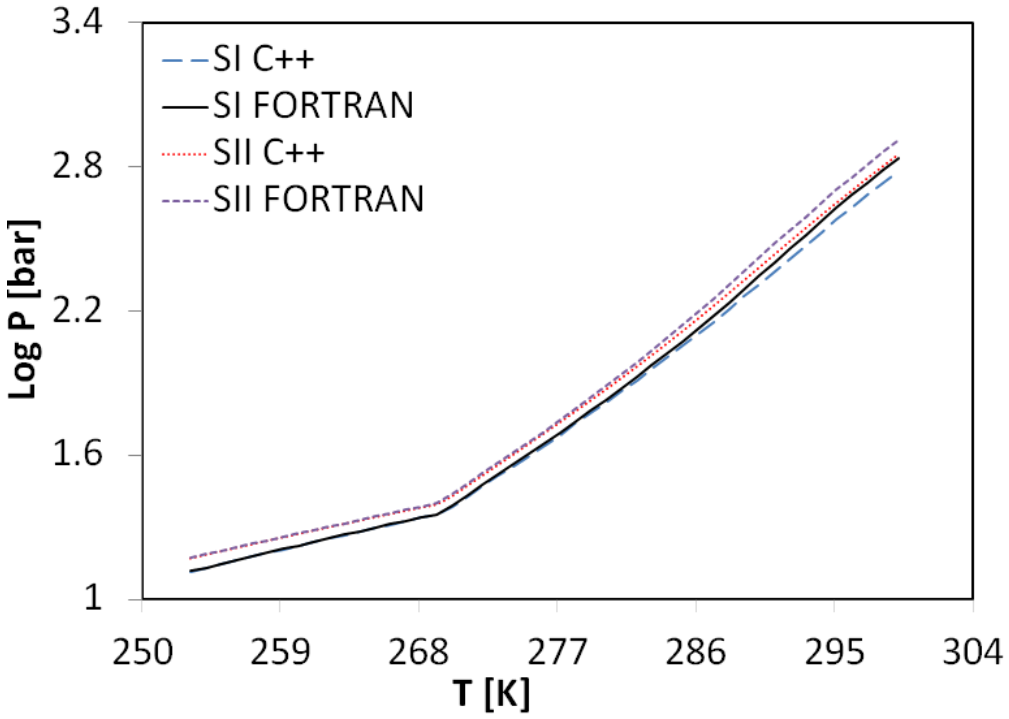

Figure 30: Comparison between Windmeier's HYCAL and the C++ implementation for a water-methane system, using the Integral Central Well potential.

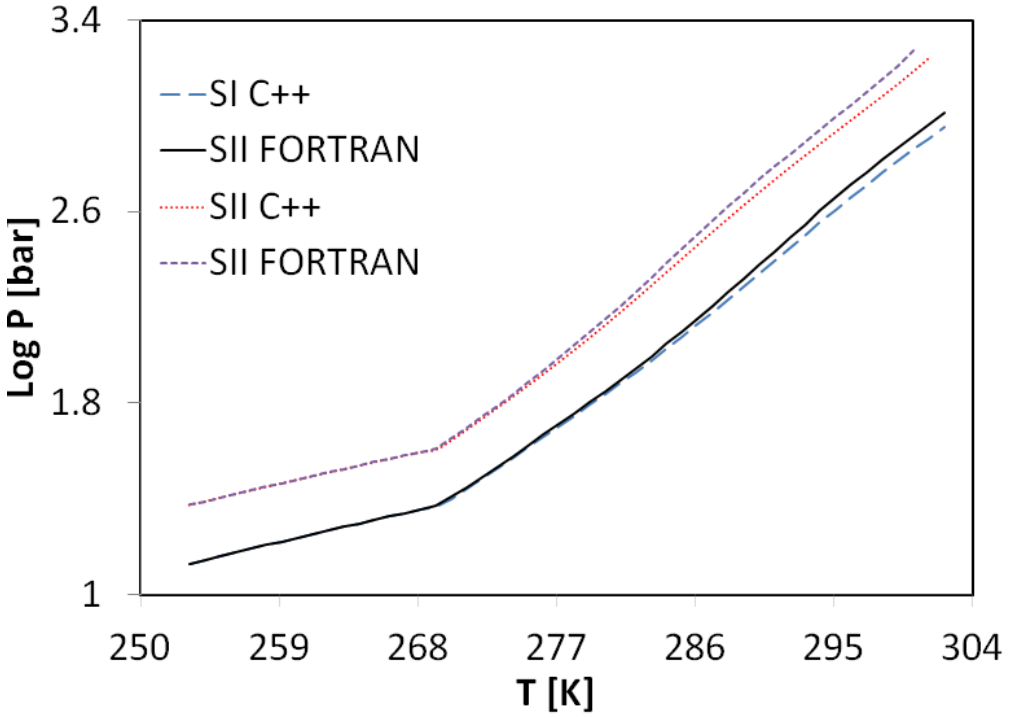

Figure 31: Comparison between Windmeier's HYCAL and C++ implementation for a water-methane system, using Kihara Potential Parameters.

9.2.2. COMPARING HYDRATES MODELS

Water and methane mixture: TP routine using PSRK model for water activity and fugacity and no solubility effects taken into consideration.

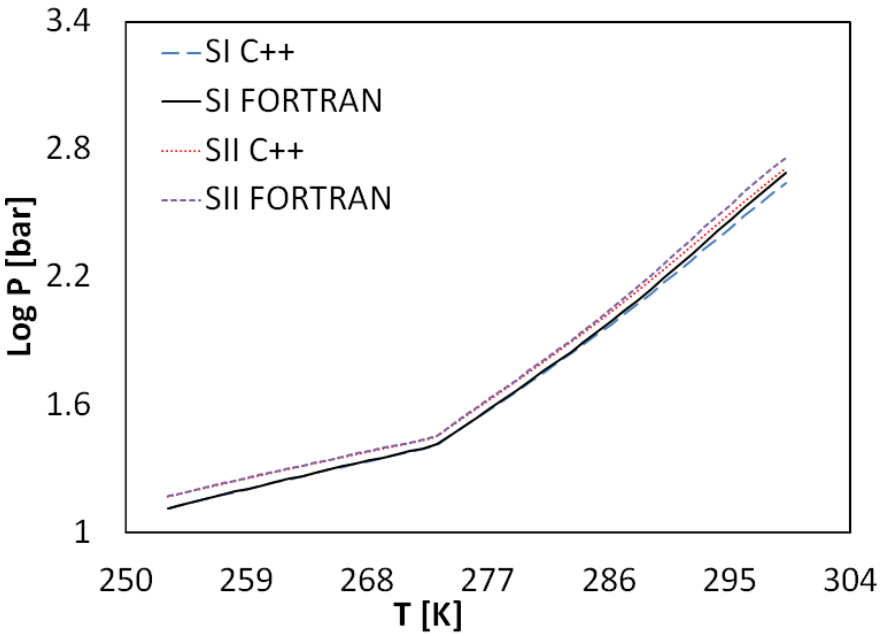

Figure 32: Comparison between hydrate models using C++ implementation for a water- methane system.

Water (x=0.9), ethanol (x=0.1) and methane mixture: TP routine using PSRK model for water activity and fugacity and no solubility effects taken into consideration.

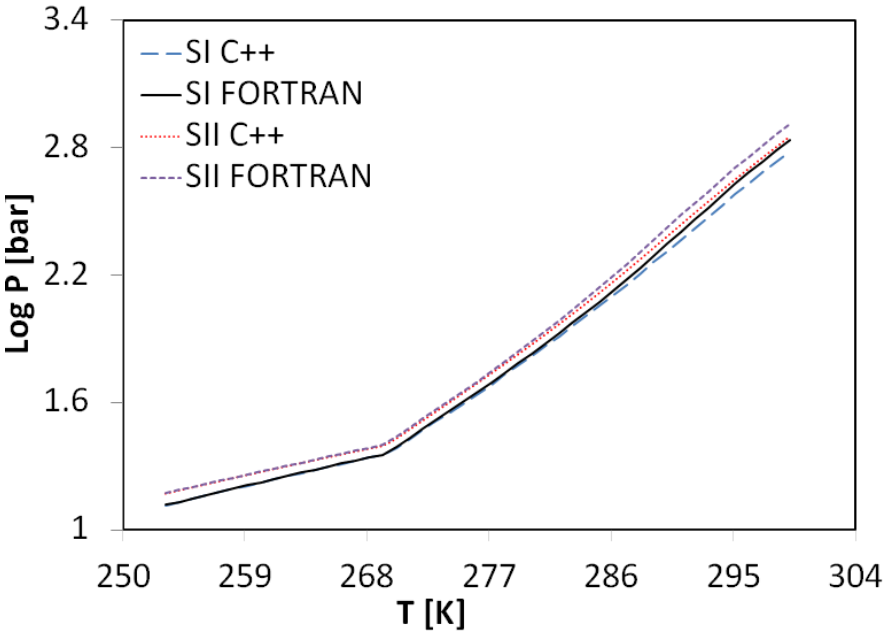

Figure 33: Comparison between hydrate models using C++ implementation for a water- methane system.

9.2.3. COMPARING C++ IMPLEMENTATION AND EXPERIMENTAL DATA

9.2.3.1. NO IHIBITORS

Water, methane, ethane and propane:

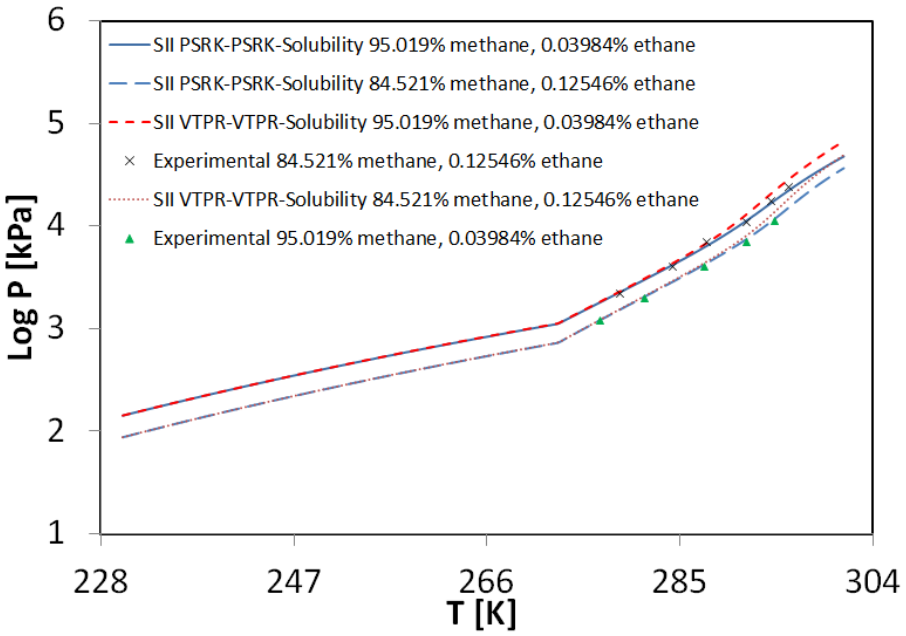

Figure 34: Comparison between C++ implementation, using Integral Central Well Potential model, and experimental data from DDB for a water-methane-ethane-propane system.

Water and hydrogen sulfide:

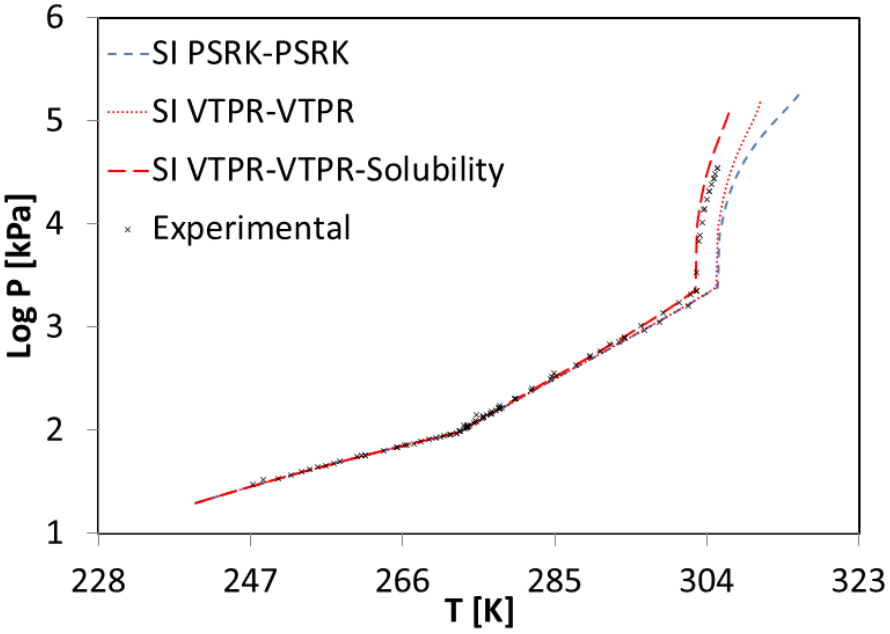

Figure 35: Comparison between C++ implementation, using the integral Central Well Potential model, and experimental data from DDB for a water-hydrogen sulfide system.

9.2.3.2. ALCOHOLS AS INHIBITOR

Water, ethanol, ethane using PSRK:

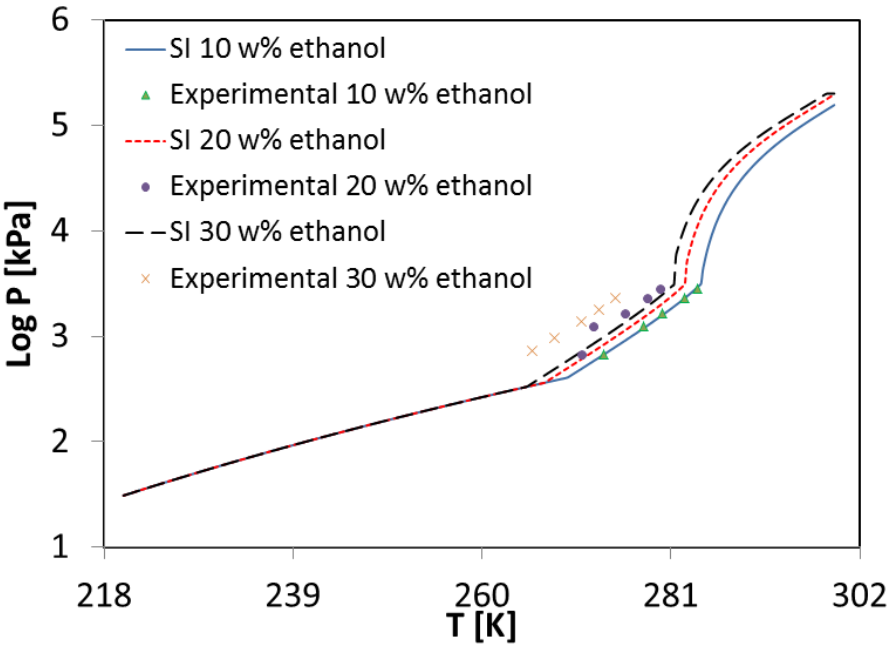

Figure 36: Comparison between C++ implementation, using the integral Central Well Potential model and PSRK, and experimental data from DDB for a water-ethanol-ethane system.

Water, ethanol, ethane using VTPR:

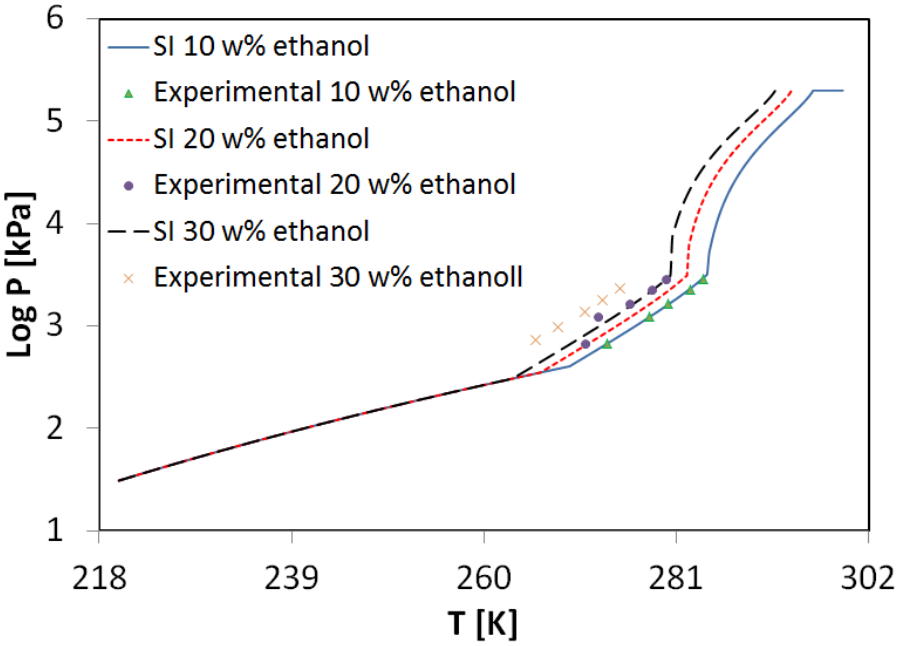

Figure 37: Comparison between C++ implementation, using the integral Central Well Potential model and PSRK, and experimental data from DDB for a water-ethanol-ethane system.

9.3.2.3. SALTS AS INHIBITOR

Water, sodium chloride, methane and nitrogen:

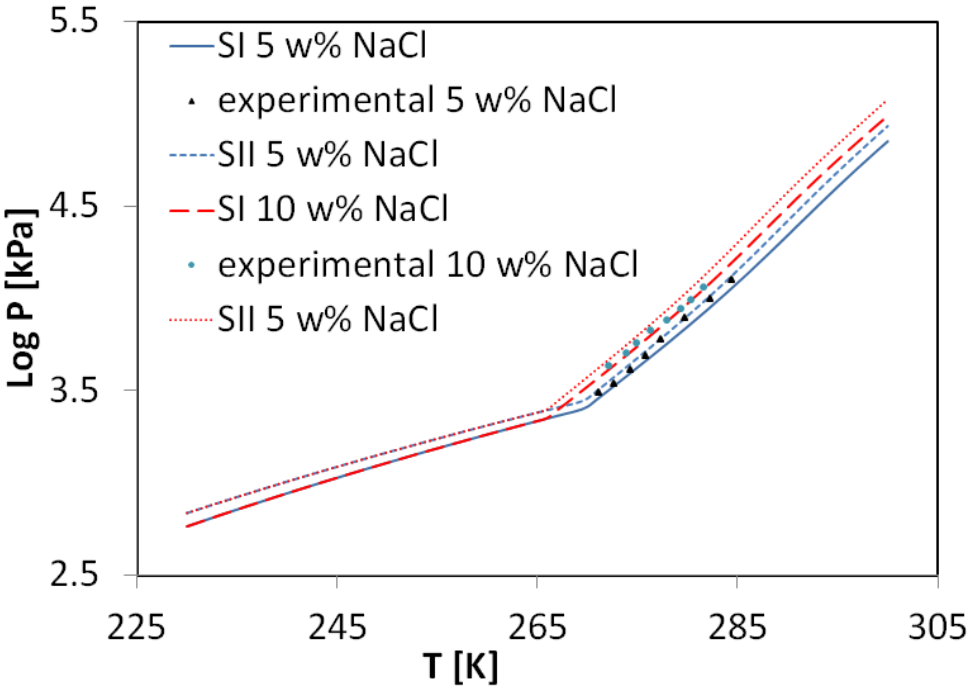

Figure 38: Comparison between C++ implementation, using the integral Central Well Potential model and PSRK, and experimental data from DDB for a water-sodium chloride-ethane system.

Water, sodium chloride, carbon dioxide and nitrogen:

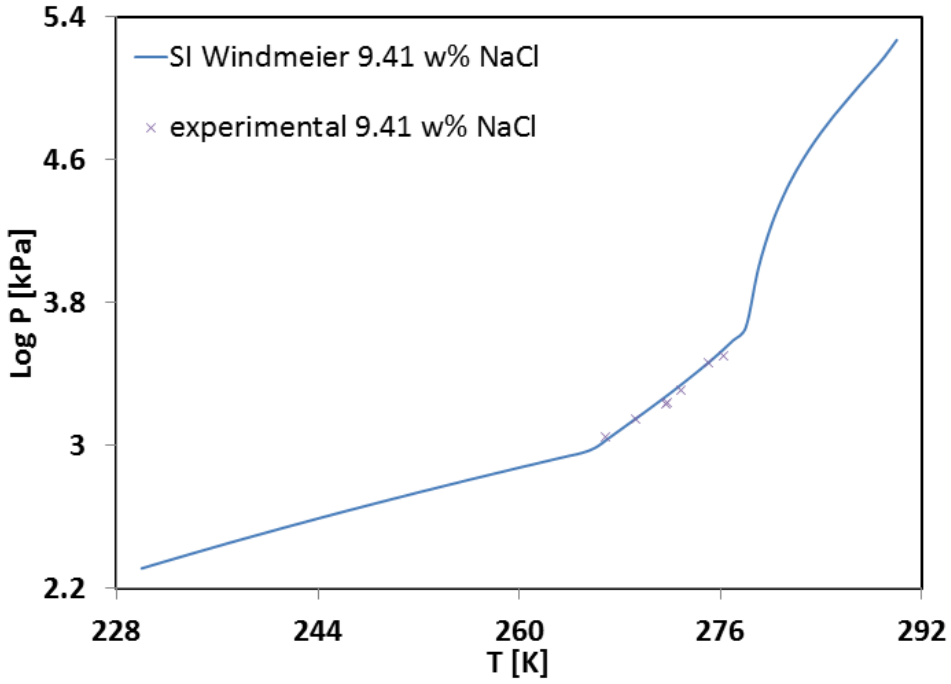

Figure 39: Comparison between C++ implementation, using the integral Central Well Potential model and PSRK, and experimental data from DDB for a water-sodium chloride-ethane system.